2. EXPLANATORY NOTES[1]

Shipboard Scientific Party[2]

Standard procedures for both drilling operations and preliminary shipboard analysis of the material recovered during the Deep Sea Drilling Project (DSDP) and Ocean Drilling Program (ODP) have been regularly amended and upgraded since drilling began in 1968. In this chapter we have assembled information that will help the reader understand the basis for our preliminary conclusions and also help the interested investigator select samples for further analysis. This information concerns only shipboard operations and analyses described in the site reports in this volume. Methods used by various investigators for shore-based analyses of Leg 119 data will be detailed in the *Scientific Results* of the Leg 119 *Proceedings of the Ocean Drilling Program.*

AUTHORSHIP OF SITE CHAPTERS

Authorship of the site report is shared among the entire shipboard scientific party, although the two co-chief scientists and the staff scientist edited and rewrote part of the material prepared by other individuals. The site chapters are organized as follows (authors are listed in alphabetical order in parentheses; no seniority is necessarily implied):

Site Summary (Barron, Hambrey, Larsen)
Background and Objectives (Barron, Larsen)
Site Geophysics (Cooper, Larsen)
Operations (Barron, Larsen)
Lithostratigraphy (Cranston, Dorn, Ehrmann, Hambrey, Jenkins, Mehl, Turner)
Basement Lithology (Alibert, Mehl)
Biostratigraphy (Baldauf, Barron, Caulet, Fryxell, Huber, Schroeder, Thierstein, Tocher, Wei)
Paleomagnetics (Keating, Sakai)
Sedimentation Rates (Baldauf, Caulet, Huber, Schroeder, Thierstein, Tocher, Wei)
Inorganic Geochemistry (Chambers, Fox, Cranston)
Organic Geochemistry (Chambers, Fox)
Biology/Oceanography (Berkowitz, Fryxell, Kang, Noh, Stockwell)
Physical Properties (Pittenger, Solheim)
Logging (Cooper, Ollier)
Seismic Stratigraphy (Cooper, Larsen)
Summary and Conclusions (Barron, Larsen)

Summary graphic, lithologic, and biostratigraphic logs, core descriptions ("barrel sheets"), and photographs of each core are grouped in the back of the book for each site.

SURVEY AND DRILLING DATA

The survey data used for specific site selections are discussed in each chapter. Short surveys using a precision echo-sounder and seismic profiles were made on *JOIDES Resolution* when approaching each site. All geophysical-survey data collected during Leg 119 are presented in the "Site Geophysics" sections of the site chapters (this volume).

Seismic-profiling systems consisted of two 80-in.^{3} water guns; one 400-in.^{3} water gun; one 300-in.^{3} air gun, having a 100-m-long hydrophone array designed at Scripps Institution of Oceanography; Bolt amplifiers; two band-pass filters; and two EDO recorders, usually recording at two different filter settings (20–300 and 30–300 Hz). The 3.5- and 12-kHz bathymetric data were displayed on Precision Depth Recorder (PDR) systems. The depths were converted on the basis of an assumed 1463 m/s sound velocity. The water depth (in meters) at each site was corrected (1) for the variation in sound velocity with depth using Matthews' (1939) tables and (2) for the depth of the hull transducer (6.8 m) below sea level. In addition, depths, when referred to the drilling-platform level, are assumed to be about 10.5 m above the water line.

DRILLING CHARACTERISTICS

Because water circulation downhole is open, cuttings were lost onto the seafloor and could not be examined. The only available information about sedimentary stratification in uncored or unrecovered intervals, other than from seismic data or wireline-logging results, is from an examination of the drill-string behavior as observed and recorded on the drilling platform. Typically, the harder the layer, the slower and more difficult it is to penetrate. A number of other factors, however, determine the rate of penetration, so it is not always possible to relate drilling time directly to the hardness of the layers. Bit weight and revolutions per minute, recorded on the drilling recorder, influence the penetration rate and bit wear.

DRILLING DEFORMATION

When the cores were split, many showed signs of significant sediment disturbance, including the convex-upward appearance of originally horizontal bands, haphazard mixing of lumps of different lithologies (mainly at the tops of cores), and the near-fluid state of some sediments recovered from tens to hundreds of meters below the seafloor. We also observed downhole contamination caused by loose, coarse materials falling from the drill hole walls. Core deformation probably occurred during one of three different steps at which the core suffered stresses sufficient to alter its physical characteristics: cutting, retrieval (with accompanying changes in pressure and temperature), and core handling on deck.

SHIPBOARD SCIENTIFIC PROCEDURES

Numbering of Sites, Holes, Cores, Sections, and Samples

ODP drill sites are numbered consecutively from the first site drilled by the *Glomar Challenger* in 1968. A site number refers

[1] Barron, J., Larsen, B., et al., 1989. *Proc. ODP, Init. Repts.*, 119: College Station, TX (Ocean Drilling Program).

[2] Shipboard Scientific Party is as given in the list of Participants preceding the contents.

to one or more holes drilled while the ship was positioned over one acoustic beacon. Multiple holes were drilled at a single site by pulling the drill pipe above the seafloor (out of the hole), moving the ship some distance from the previous hole, and then drilling another hole.

For all ODP drill sites, a letter suffix distinguishes each hole drilled at the same site. For example, the first hole drilled was assigned the site number modified by the suffix A, the second hole has the site number and suffix B, and so forth. Note that this procedure differs slightly from that used by DSDP (Sites 1 through 624), but prevents ambiguity between site- and hole-number designations. We needed, for sampling purposes, to distinguish among holes drilled at a site, because recovered sediments or rocks from different holes usually did not come from equivalent positions in the stratigraphic column.

Investigators measured the cored interval in meters below seafloor (mbsf). The depth interval for each core ranges from the depth below the seafloor that the coring operation began to the depth that the coring operation ended. For example, each coring interval is usually 9.7 m long (the nominal capacity of a core barrel). However, the coring intervals may be shorter and may not necessarily be adjacent to each other, but they may be separated by drilled intervals. In soft sediments, the drill string could be "washed ahead" with the core barrel in place, but not recovering sediments, by pumping water down the pipe at high pressure to wash the sediment out of the way of the bit and up the space between the drill pipe and wall of the hole. If thin, hard-rock layers are present, "spotty" sampling of these resistant layers within the washed interval may occur and thus result in a cored interval >9.7 m. When drilling hard rock, a center bit may be used instead of the core barrel if drilling must continue without core recovery.

Cores taken from a hole are numbered serially from the top of the hole downward. Core numbers and their associated cored intervals in meters below seafloor usually are unique in a given hole; however, this may not be true if an interval had to be cored twice, owing to caving of cuttings or other hole problems. Nominally, a fully-recovered core consists of 9.7 m of rock or sediment contained in a plastic liner (6.6-cm internal diameter) plus about 0.2 m (without a plastic liner) in the core catcher. The core catcher is a device at the bottom of the core barrel that prevents the core from sliding out when the barrel is being retrieved from the hole.

A recovered core was divided into 1.5-m sections that are numbered serially from the top (Fig. 1). When full recovery was obtained, the sections were numbered from 1 through 7, with the last section possibly being shorter than 1.5 m (rarely, an unusually long core may require more than seven sections). When less than full recovery was obtained, there will be as many sections as needed to accommodate the length of the core recovered. For example, 4 m of core would be divided into two 1.5-m sections and one 1-m section. If cores were fragmented (recovery less than 100%), sections are numbered serially and intervening sections are noted as void, whether shipboard scientists believe that the fragments were contiguous *in situ* or not. Material recovered from the core catcher was placed below the last section when the core was described and labeled core catcher (CC). In sedimentary cores, it was treated as a separate section. Scientists completing visual core descriptions (VCD) reported each section as a physical unit; one or more lithologic boundaries may occur anywhere within this physical unit and were not considered when the core was assigned sections.

A recovered basalt core also was cut into 1.5-m sections and numbered serially; however, each piece of rock then was assigned a number (fragments of a single piece were assigned a single number, with individual fragments identified alphabetically). The core-catcher sample was placed at the bottom of the last section and was treated as part of the last section rather than separately. Scientists completing visual core descriptions described each lithologic unit, noting core and section boundaries only as physical reference points.

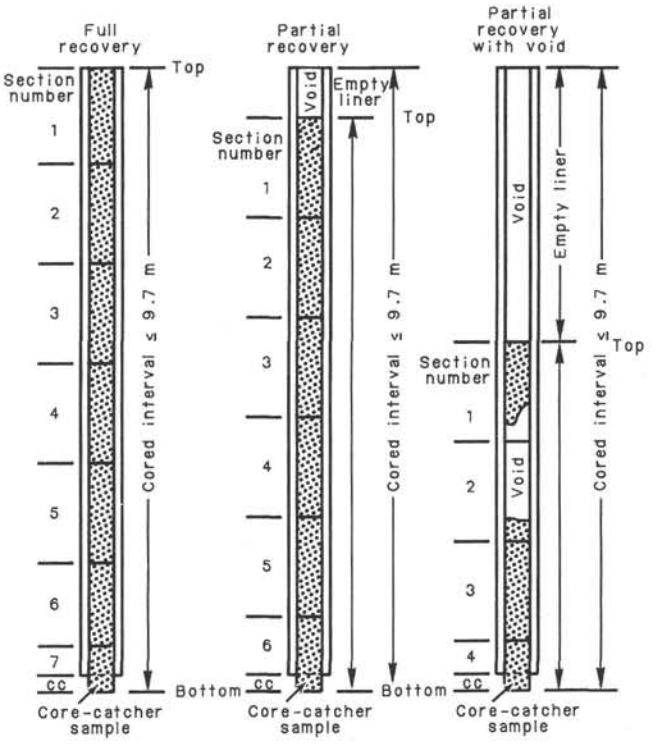

Figure 1. Diagram showing procedure for cutting and labeling core sections.

When, as is usually the case, the recovered core was shorter than the cored interval, the top of the core was equated with the top of the cored interval by convention in order to achieve consistency in handling analytical data derived from the cores. Samples removed from the cores were designated by the distance measured in centimeters from the top of the section to the top and bottom of each sample removed from that section. In curated hard-rock sections, sturdy plastic spacers were placed between pieces that did not fit together in order to protect them from damage in transit and in storage. Therefore, the centimeter interval noted for a hard-rock sample has no direct relationship to that sample's depth within the cored interval, but is only a physical reference to the sample's location within the curated core.

A full identification number for a sample consists of the following information: Leg, Site, Hole, Core Number, Core Type, Section Number, Interval in centimeters measured from the top of section, and Piece Number (used for hard rock only). For example, Sample "119-736A-5R-3, 100–102 cm" would be a sediment sample removed from the interval between 100 and 102 cm below the top of Section 3, Core 5 (R designates that this core was taken with the RCB) of Hole 736A during Leg 119.

All ODP core and sample identifiers indicate core type. The following abbreviations are used: R = rotary core barrel (RCB); H = hydraulic piston core (HPC) and advanced piston core (APC); P = pressure core barrel; X = extended core barrel (XCB); B = drill-bit recovery; C = center-bit recovery; I = *in-situ* water sample; S = sidewall sample; W = wash-core recovery; N = Navidrill core; and M = miscellaneous material. Only RCB, HPC, XCB, and wash cores were drilled on ODP Leg 119.

Core Handling

As soon as a core was retrieved on deck during Leg 119, a sample was taken from the core catcher and given to the paleontological laboratory for an initial age assessment. The core was then placed on the long horizontal rack, and gas samples were taken by piercing the core liner and withdrawing gas into a vacuum-tube sampler. Voids within the core were sought as sites for gas sampling. Some of the gas samples were stored for shore-base study, but others were analyzed immediately as part of the shipboard safety and pollution prevention program. Next, the core was marked into section lengths, each section labeled, and the core cut into sections. Interstitial-water (IW), organic geochemistry (OG), and physical-properties (PP) whole-round samples then were taken. Each section was sealed at the top and bottom by gluing on color-coded plastic caps, blue to identify the top of a section and clear for the bottom. A yellow cap was placed on section ends from which a whole-round sample had been removed. Similarly, red caps were placed on section ends from which an OG sample had been taken. The caps were usually attached to the liner by coating the end liner and the inside rim of the cap with acetone, and the caps were taped to the liners.

Then the cores were carried into the laboratory, where the sections were again labeled, using an engraver to mark the full designation of the section. The length of the core in each section and the core-catcher sample were measured to the nearest centimeter; this information was logged into the shipboard core log data-base program.

The cores then were allowed to warm to room temperature (approximately 4 hr) before they were split. During this time, the whole-round sections were run through the GRAPE device (estimating the bulk density and porosity see following text; Boyce, 1976), the *P*-wave-logger simultaneous determination of sonic velocity, and the pass-through cryogenic magnetometer (see following text). After the core temperatures equilibrated, thermal-conductivity measurements were made immediately before the cores were split.

Cores of relatively soft material were split lengthwise into working and archive halves. The softer cores were split with a wire or saw, depending on the degree of induration. Harder cores were split with a band saw or diamond saw. As cores on Leg 119 were split with wire from the bottom to top, older material possibly could be transported up the core on the split face of each section. Investigators were aware that the very near-surface part of the split core could be contaminated and avoided using this part.

The working half was sampled for both shipboard and shore-based laboratory studies. Each extracted sample was then logged in the sampling computer program by the location and the name of the investigator receiving the sample. Records of all removed samples are kept by the curator at ODP. The extracted samples were sealed in plastic vials or bags and labeled. Samples were routinely taken for shipboard analysis of water content by gravimetric analysis, for percentage of calcium carbonate present (coulometric determination), and for other purposes. Many of these data are reported in the site chapters.

The archive half was described visually. Smear slides and shipboard grain-size analysis were made from samples taken from the archive half, and they were supplemented by thin sections taken from the working half. The archive half then was photographed with both black-and-white and color film, a whole core at a time, and close-ups were made as requested by the scientists.

Both halves of the core then were put into labeled plastic tubes, which were sealed and transferred to cold-storage space aboard the drilling vessel. Leg 119 cores were transferred from the ship by refrigerated vans to cold storage at the East Coast Repository at Lamont-Doherty Geological Observatory, Palisades, New York.

CORE DESCRIPTION FORMS (BARREL SHEETS)

The core description form (Fig. 2), or barrel sheet, summarizes the data obtained during shipboard analysis of each core. The following discussion explains the ODP conventions used in compiling each part of the core description form and the exceptions to these procedures adopted by Leg 119 scientists.

Core Designation

Cores are designated using site, hole, and core number and type as previously discussed (see "Numbering of Sites, Holes, Cores, Sections, and Samples" section, this chapter). In addition, the cored interval is specified in terms of meters below seafloor. On Leg 119, these depths were based on the drill-pipe measurements, as reported by the SEDCO coring technician and the ODP operations superintendent.

Age Data

Microfossil abundance, preservation, and zone assignment, as determined by the shipboard paleontologists, appear on the core description form under the heading "Biostratigraphic Zone/Fossil Character." The geologic age determined from the paleontological results is shown in the "Time-Rock Unit" column. Detailed information on the zonations and terms used to report abundance and preservation appear in the "Biostratigraphy" section (this chapter).

Paleomagnetic, Physical-Property, and Chemical Data

Columns are provided on the core description form to record paleomagnetic results, location of physical-properties samples (density, porosity, and thermal conductivity), and chemical data (percentage of $CaCO_3$ determined using coulometrics). Additional information on shipboard procedures for collecting these types of data appears in the "Paleomagnetics," "Inorganic Geochemistry," and "Physical Properties" sections (this chapter).

Graphic Lithology Column

The lithologic classification scheme presented here is represented graphically on the core description forms using the symbols illustrated in Figure 3. Modifications and additions made to the graphic lithology representation scheme recommended by the JOIDES Sedimentary Petrology and Physical Properties Panel are discussed in the "Lithologic Description" section (this chapter).

Sediment Disturbance

The coring technique, which involved a 25-cm-diameter bit with a 6-cm-diameter core opening, may result in extreme disturbance of the recovered core material. This is illustrated in the "Drilling Disturbance" column on the core description form using the symbols in Figure 4, as described in the following disturbance categories recognized for soft and firm sediments:

1. Slightly deformed: bedding contacts are slightly bent.
2. Moderately deformed: bedding contacts have undergone extreme bowing.
3. Highly deformed: bedding is completely disturbed, sometimes showing symmetrical diapirlike structures.
4. Soupy: intervals are water-saturated and have lost all aspects of original bedding.

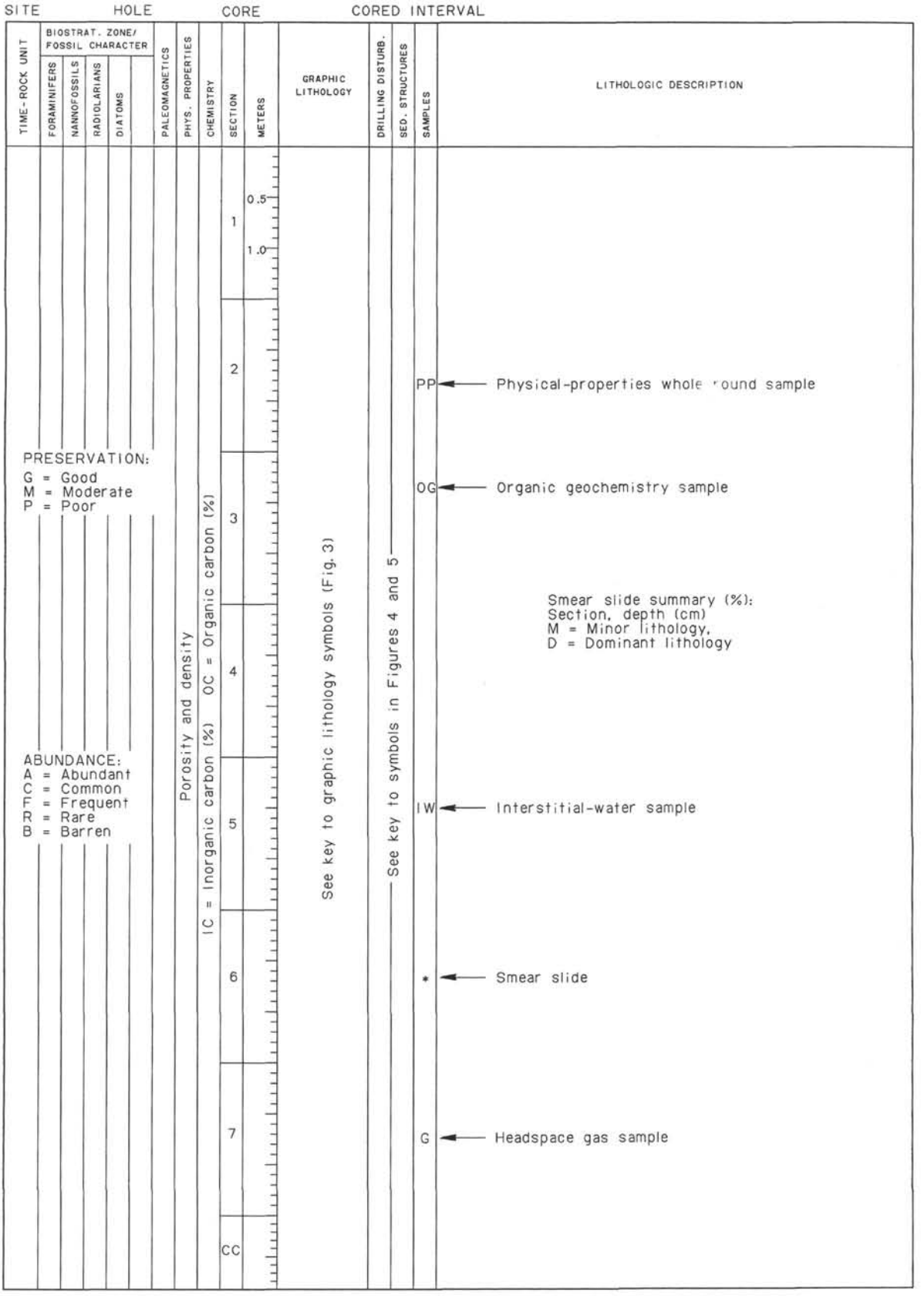

Figure 2. Core description form (barrel sheet) used for sediments and sedimentary rocks.

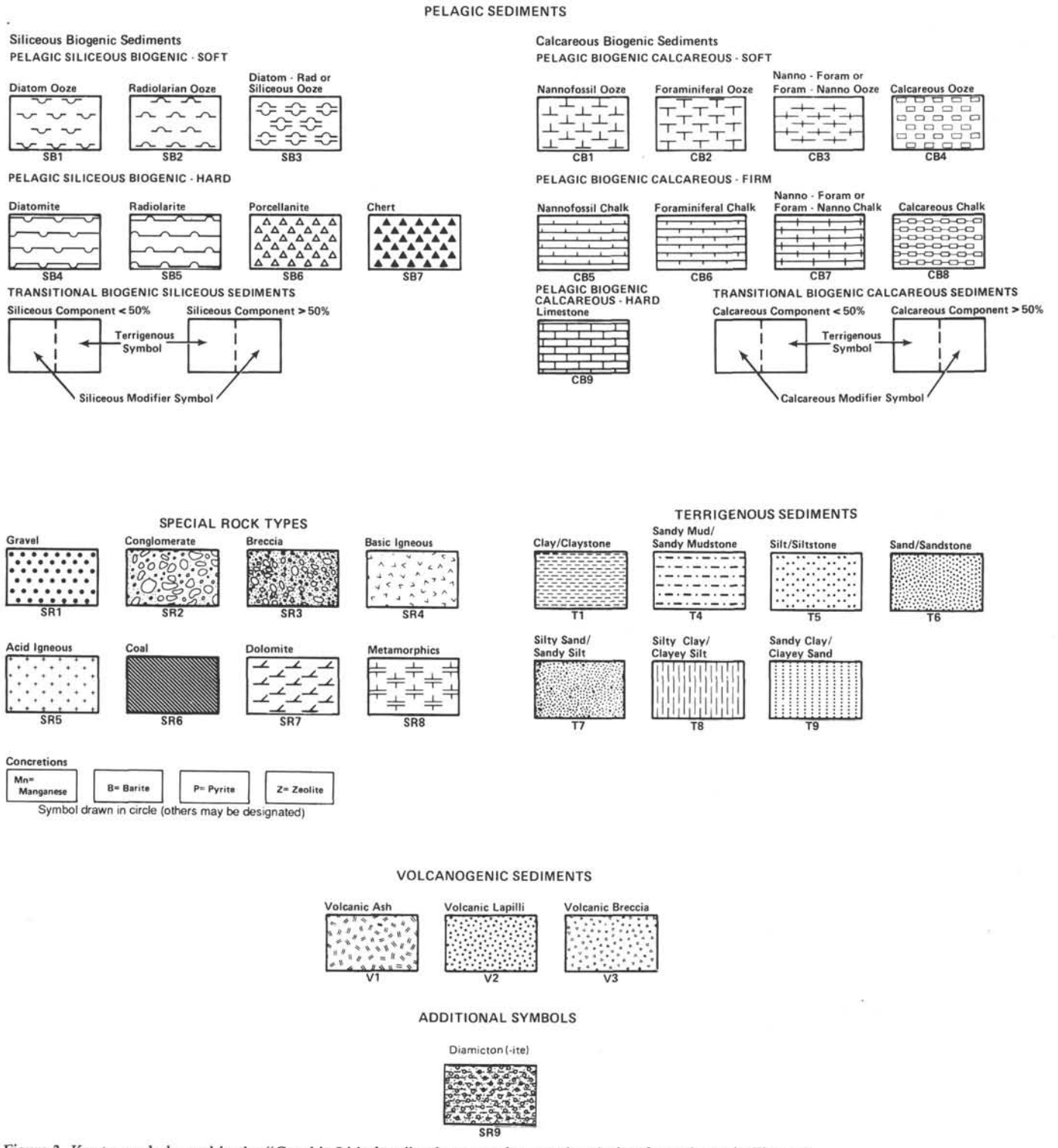

Figure 3. Key to symbols used in the "Graphic Lithology" column on the core description form shown in Figure 2.

The following categories are used to describe the degree of fracturing in hard sediments and igneous and metamorphic rocks (Fig. 4):

1. Slightly fractured: core pieces are in place and have very little drilling slurry or breccia.

2. Moderately fragmented: core pieces are in place or partly displaced, but original orientation is preserved or recognizable; drilling slurry may surround fragments.

3. Highly fragmented: pieces are from interval cored and probably in correct stratigraphic sequence (although they may not represent the entire section), but original orientation is totally lost.

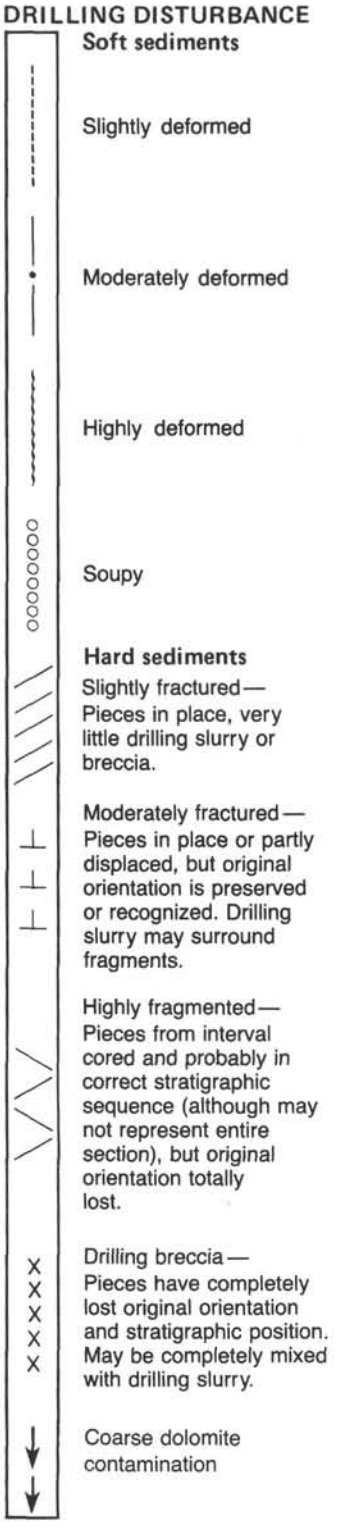

Figure 4. Drilling disturbance symbols used on Leg 119 core description forms.

4. Drilling breccia: core pieces have completely lost their original orientation and stratigraphic position and may be completely mixed with drilling slurry.

Downhole contamination resulted from loose materials falling from the drill hole walls. Most commonly it appeared at the top of a core as hydrodynamically well-sorted gravel or coarse sand up to 1 m thick, typically with multiple layering and lumps of mixed-gravel/soft-sediment pug. A convex conical drilling surface usually lies below the sharp base of the gravel. Isolated pieces of gravel contamination also may occur alongside the core liner away from the core top.

Sedimentary Structures

In the soft and even in some harder sedimentary cores, distinguishing between natural structures and those created by the coring process may be extremely difficult. However, where such structures were observed, they are indicated on the "Sedimentary Structure" column of the core description form. A key to the structural symbols used on Leg 119 is given in Figure 5.

Samples

The position of samples taken from each core for shipboard analysis is indicated in the "Samples" column in the core description form. An asterisk (*) indicates the location of smear slide samples. The symbols IW, OG, and PP designate whole-round interstitial-water, frozen organic geochemistry, and physical-properties samples, respectively.

Although not indicated in the "Samples" column, the position of samples for routine physical-property and coulometric carbonate analyses are indicated by a square in the "Physical Properties" and "Chemistry" columns (these samples are from the working half of the core and generally, although not always, correspond to smear slide locations in the archive half).

Shipboard paleontologists generally based their age determinations on core-catcher samples, although additional samples from other parts of the core have been examined when required.

Lithologic Description

The lithologic description that appears on each core description form consists of two parts: (1) a brief summary of the major lithologies observed in a given core in order of importance, followed by a description of sedimentary structures and features, and (2) a description of minor lithologies observed in the core, including data on color, occurrence in the core, and significant features.

Smear Slide Summary

A table summarizing smear slide and thin-section data, if available, appears on each core description form. The section and interval from which the sample was taken are noted, as well as identification as a dominant (D) or minor (M) lithology in the core. The percentage of all identified components (totaling 100%) is listed. As explained in the following "Sediment Classification" section (this chapter), these data are used to classify the recovered material.

Sediment Measurements

Smear Slide Examination

Semiquantitative data of low accuracy was compiled on the composition and texture of the finer sediments. Samples of approximately 10 mg were mounted in Canada balsam and examined using petrological microscopes. The percentage of fossil and mineral components, as well as size classes (sand/silt/clay), were estimated visually. Special problems were encountered in differentiating quartz and fresh, untwinned feldspar; in estimating clay percentage; in truly representing the coarser sand fractions during preparation; and in disagregating the clay fraction of the semilithified sediments. Estimated levels of accuracy are $\pm 10\%$ for major, easily identifiable mineral phases and $\pm 1/2$ the estimated percentage for minor phases.

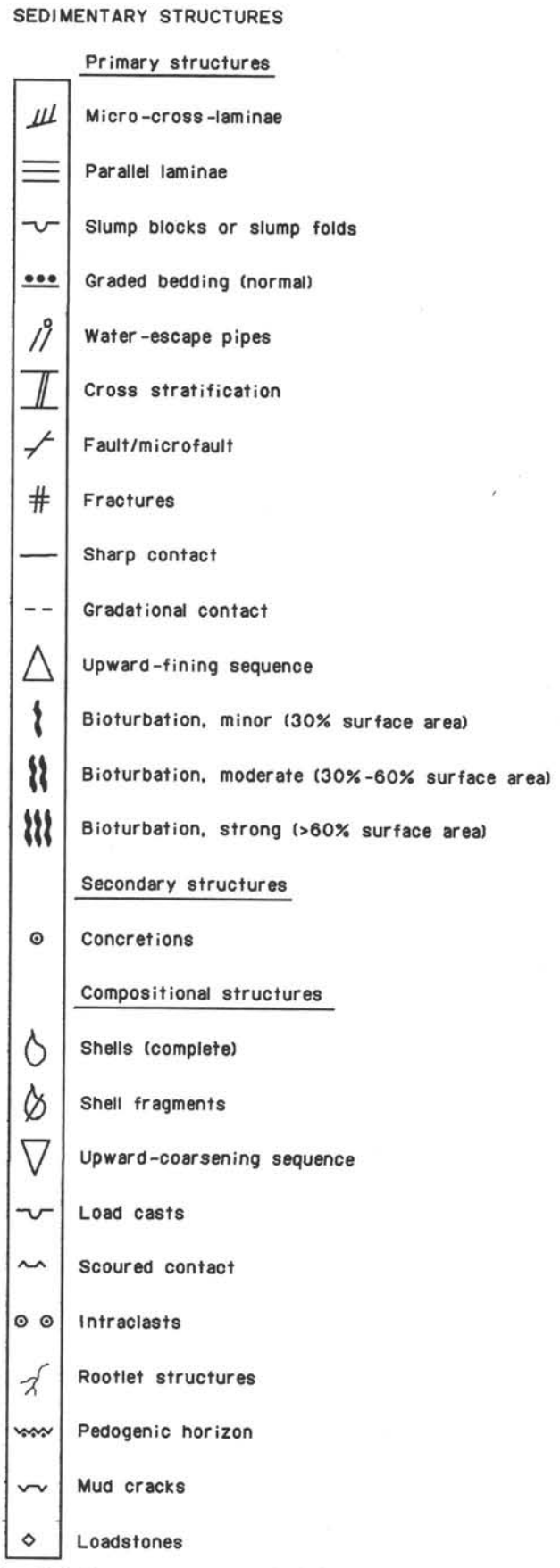

Figure 5. Sedimentary structure symbols for sediments and sedimentary rocks.

Grain Size

For routine assignment of sediments to textural classes, grain size was estimated visually from the core material and smear slides. For the finer, soft sediments, a Lasentec Lab-Tec 100 particle-size analyzer was tested and used (for the first time on this leg) to provide data on the sand/silt/clay ratio and mean grain size. In this instrument a stirred, horizontally rotating, dilute suspension of the sediment is scanned in a vertical plane by a finely focused laser-diode beam. Individual particle cross sections are measured from the duration of the back-scattering events. The analyses are rapid and appear to be accurate to $\pm 5\%$ (at full range) in the range of 1–125 μm under controlled operation.

A total of 10^4 particle counts is obtained from sediment samples of about 100 mg, so the data are statistically sound. However, special procedures are required to minimize clay flocculation and the disintegration of delicate grains. Measurements are not accurate with dull, black particles (e.g., MnO_2-coated grains). Furthermore, sediments with sand-sized grains could not be kept in suspension at the level of the scanning beam. To convert the raw size/frequency data (which are dependent on the optical cross section of each size class) to traditional sedimentologic size/weight percentage data, compensation factors must be applied. In general these factors correspond to each class median size, but some sediment types require calibration through sieve and pipette analyses (e.g., hollow grains in biogenic ooze). Most of these problems could not be solved aboard ship. Therefore, these grain-size analyses are of limited value and give only a rough estimate on the real grain-size distribution of the sediments.

Sediment Classification

The new classification scheme for the Ocean Drilling Program by Mazzullo et al. (1987), partly given below, was used during Leg 119 for the first time. However, the following amendments and comments were included.

1. The term *neritic* in the scheme has been substituted by *calciclastic*. The use of neritic for nonpelagic carbonate grains differs significantly from its use elsewhere (Bates and Jackson, 1980) and may cause misunderstandings.
2. The term *mudstone* in the scheme designating fine-grained limestone is unfortunate, because this term designates indurated, fine-grained, terrigenous sediments in previous ODP schemes and general usage. This usage of mudstone in the new scheme is replaced by *calcilutite*.
3. Clastic sediments of volcanic provenance are described in the same fashion as siliciclastic sediment, noting the dominant composition of the volcanic grains.
4. The ODP classification does not adequately address nonsorted or poorly sorted siliciclastic sediments, such as those characterized by tills or debris flows. For this type of sediment, we applied the terms *diamicton* (unlithified) or *diamictite* (lithified) proposed by Flint et al. (1960).
5. The proper use of Shepard's (1954) ternary diagram (Fig. 6) for naming mixtures of sand, silt, and clay requires grain-size analysis. The addition of a Lab-Tec particle analyzer to the shipboard sediment laboratory made this analysis possible for some fine-grained sediments, but not for all. Note, however, that the use of the sediment names in Shepard's (1954) diagram differs significantly from common usage. Especially of note is the influence of the clay content on properties, and thus the naming is underestimated by the scheme.

Granular Sediments

The following types of grains can be found in granular sediments: (1) pelagic, (2) calciclastic, (3) siliciclastic, and (4) volca-

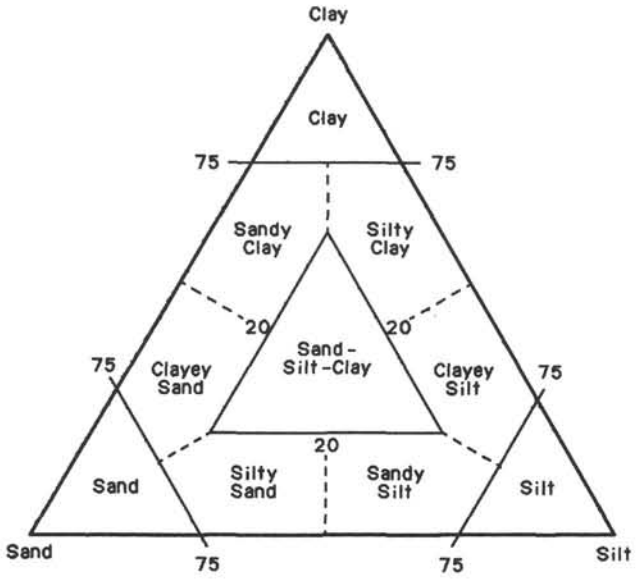

Figure 6. Ternary diagram showing principal names for siliciclastic sediments (from Shepard, 1954).

niclastic (Fig. 7). Pelagic grains are composed of the organic debris of open-marine, siliceous, and calcareous microfauna and microflora (e.g., radiolarians, nannofossils) and associated organisms. Calciclastic grains are composed of coarse-grained calcareous debris and fine-grained calcareous grains of nonpelagic origin (e.g., micrite). Siliciclastic grains are composed of mineral and rock fragments derived from igneous, sedimentary, and metamorphic rocks. Volcaniclastic grains are composed of rock fragments and minerals derived from volcanic sources.

Variations in the relative proportions of these four grain types define five major classes of granular sediments: (1) pelagic, (2) calciclastic, (3) siliciclastic, (4) volcaniclastic, and (5) mixed sediments (Fig. 7).

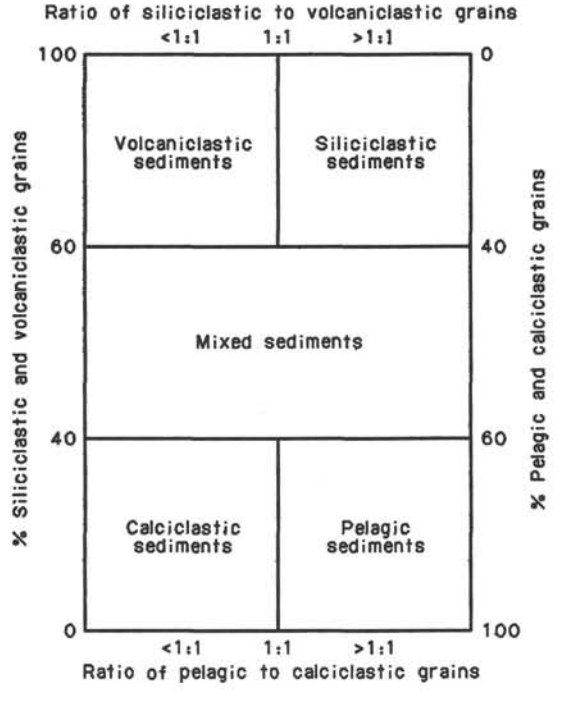

Figure 7. Diagram showing classes of granular sediments.

1. Pelagic sediments are composed of >60% pelagic and calciclastic grains and <40% siliciclastic and volcaniclastic grains. They also contain a higher proportion of pelagic than calciclastic grains.
2. Calciclastic sediments are composed of >60% calciclastic and pelagic grains and <40% siliciclastic and volcaniclastic grains. They contain a higher proportion of calciclastic than pelagic grains.
3. Siliciclastic sediments are composed of >60% siliciclastic and volcaniclastic grains and <40% pelagic and calciclastic grains. They contain a higher proportion of siliciclastic than volcaniclastic grains.
4. Volcaniclastic sediments are composed of >60% siliciclastic and volcaniclastic grains and <40% pelagic and calciclastic grains. They contain a higher proportion of volcaniclastic than siliciclastic grains. This class includes epiclastic sediments (volcanic detritus produced by erosion of volcanic rocks by wind, water, and ice), pyroclastic sediments (products of the degassing of magmas), and hydroclastic sediments (products of volcanic glass granulation by steam explosions).
5. Mixed sediments are composed of 40%–60% siliciclastic and volcaniclastic grains and 40%–60% pelagic and calciclastic grains.

A granular sediment can be classified by designating a principal name and major and minor modifiers. The principal name of a granular sediment defines its granular-sediment class; the major and minor modifiers describe the texture, composition, fabric, and/or roundness of the grains themselves (see Tables 1 and 2 and Appendix A for details). For a description of sedimentary structures, see Figure 5.

Genetic Classification of Glaciogenic Sediments

In the site reports for Prydz Bay, glaciogenic sediments, characterized by poor sorting, have been described using nongenetic terms. In environmental interpretation, several genetic classifications of glaciogenic sediments are used, particularly in the marine environment. The following definitions are adapted from Barrett et al. (in press) and Hambrey et al. (in press). These definnitions also reflect the work of the INQUA Commission on the Genesis and Lithology of Glacial Deposits (Dreimanis, 1979) and from GICP Project 38 Pre-Pleistocene Tillites (Hambrey and Harland, 1981):

1. Lodgement till: deposited by active "plastering on" of subglacial debris by grounded ice (which may or may not be below sea level).
2. Melt-out till (subglacial): deposited from the base of a grounded glacier by melt-out processes (differs from lodgement till because the ice is relatively inactive when the debris is released).
3. Basal till: embraces both lodgement and melt-out tills.
4. Waterlaid till: deposition by continuous rain out of basal glacial debris from a floating glacier tongue just seaward of grounding line but without significant reworking by bottom currents or by slumping.
5. Proximal glaciomarine sediment: deposition of marine sediments of terrigenous and biogenic origin (e.g., sands, muds, and diatom ooze), with the addition of a high proportion of ice-rafted material following calving of either a floating or grounded glacier tongue.
6. Distal glaciomarine sediment: deposition of predominantly marine sediments with the addition of a minor ice-rafted component distal from the ice margin.

Table 1. Outline of the granular-sediment classification scheme, Leg 119. See Appendix A for details.

Sediment class	Major modifiers	Principal names	Minor modifiers
Pelagic	1. Composition of pelagic and calciclastic grains present in major amounts. 2. Texture of clastic grains present in major amounts	1. Ooze 2. Chalk 3. Limestone 4. Radiolarite 5. Diatomite 6. Spicularite 7. Chert	1. Composition of pelagic and calciclastic grains present in minor amounts 2. Texture of clastic grains present in minor amounts
Calciclastic	1. Composition of claciclastic and pelagic grains present in major amounts 2. Texture of clastic grains present in major amounts	1. Boundstone 2. Grainstone 3. Packstone 4. Wackestone 5. Floatstone 6. Rudstone 7. Calcilutite	1. Composition of calciclastic and pelagic grains present in minor amounts 2. Texture of clastic grains present in minor amounts
Siliciclastic	1. Composition of all grains present in major amounts 2. Grain fabric (gravels only) 3. Grain shape (optional) 4. Sediment color (optional)	1. Gravel 2. Sand 3. Silt 4. Clay 5. Diamictite (etc.)	1. Composition of all grains present in minor amounts 2. Texture and composition of siliciclastic grains present as matrix (for coarse-grained clastic sediments)
Volcaniclastic	1. Composition of all volcaniclasts present in major amounts 2. Composition of all pelagic and calciclastic grains present in major amounts 3. Texture of siliciclastic grains present in major amounts	1. Breccia 2. Lapilli 3. Ash/tuff 4. Volcanic sand (etc.)	1. Composition of all volcaniclasts present in minor amounts 2. Composition of all calciclastic and pelagic grains present in minor amounts 3. Texture of siliciclastic grains present in minor amounts
Mixed	1. Composition of calciclastic and pelagic grains present in major amounts 2. Texture of clastic grains present in major amounts	1. Mixed sediments	1. Composition of calciclastic and pelagic grains present in minor amounts 2. Texture of calciclastic grains present in minor amounts

The terms *proximal* and *distal* refer essentially to the nature of the deposit and ignore such influences as iceberg drift pathways. Thus, terms concerning distance from the glacier may be ambiguous if the currents concentrated icebergs and, therefore, deposition along certain paths. In addition, the degree to which the glacial component is diluted by marine sediments will be a significant factor.

Basement Description Convention

Visual Core Descriptions

Igneous rock representation on barrel sheets is too compressed to provide adequate information for potential sampling. Consequently, visual core description forms, modified from those used aboard ship, were used for more complete graphic representation. Copies of the visual core description forms, as well as other prime data collected during Leg 119, are available on microfilm at all three ODP repositories.

Core Curation and Shipboard Sampling

Igneous rocks were split into archive and working halves using a rock saw with a diamond blade. The curatorial technician decided on the orientation of each cut so as to preserve unique features and/or to expose important structures. The archive half was described and samples for shipboard and shore-based analyses were removed from the working half.

On a typical igneous rock core description form (Fig. 8), the column is a visual representation of the archive half. A horizontal line across the entire width of the column denotes a plastic spacer glued between rock pieces inside the liner. Each piece is numbered sequentially from the top of each section, beginning with number 1. Pieces are labeled on the rounded, not sawed, surface. Pieces that can be fitted together (reassembled like a jigsaw puzzle) are assigned the same number, but they are lettered consecutively (e.g., 1A, 1B, 1C, etc.). Spacers are placed between pieces with different numbers, but not between those with different letters and the same number. Presence of a spacer may represent a substantial interval of no recovery.

Whenever the original unsplit piece is sufficiently large, the top and bottom can be distinguished before removal from the core liner (i.e., the piece could not have rotated top to bottom about a horizontal axis in the liner during drilling). To maintain this distinction, an arrow was added to the label pointing to the top of the section. We were careful to maintain orientation during the splitting and labeling processes. Oriented pieces are indicated on the description forms by upward-pointing arrows to the right of the piece. Because pieces were free to turn about a vertical axis during drilling, azimuthal orientation was not possible.

After the core was split, we sampled it for shipboard physical-properties, magnetics, and thin-section studies. Samples were taken from the working half for physical-properties measurements (index properties, GRAPE density, and velocity). On the visual core description forms, the type of measurement and approximate sample interval are indicated in the column headed "Shipboard Studies," using the following notations:

1. M = magnetic measurements
2. T = thin section
3. P = physical-properties measurements.

Table 2. Grain-size categories used for classification of terrigenous sediments (from Wentworth, 1922).

Grain size (mm)	Grain size (μm)	Grain size (φ)	Wentworth size class
		−0.20	
4096		−0.12	
1024		−0.10	Boulder (−0.8 to −0.12 φ)
256		−0.8	Cobble (−0.6 to −0.8 φ)
64		−0.6	
16		−4	Pebble (−0.2 to −0.6 φ)
4		−2	
3.36		−1.75	
2.83		−1.5	Granule
2.38		−1.25	
2.00		−1.0	
1.68		−0.75	
1.41		−0.5	Very coarse sand
1.19		−0.25	
1.00		0.0	
0.84		0.25	
0.71		0.5	Coarse sand
0.59		0.75	
1/2 0.50	500	1.0	
0.42	420	1.25	
0.35	350	1.5	Medium sand
0.30	300	1.75	
1/4 0.25	250	2.0	
0.210	210	2.25	
0.177	177	2.5	Fine sand
0.149	149	2.75	
1/8 0.125	125	3.0	
0.105	105	3.25	
0.088	88	3.5	Very fine sand
0.074	74	3.75	
1/16 0.0625	63	4.0	
0.053	53	4.25	
0.044	44	4.5	Coarse silt
0.037	37	4.75	
1/32 0.031	31	5.0	
1/64 0.0156	15.6	6.0	Medium silt
1/128 0.0078	7.8	7.0	Fine silt
			Very fine silt
1/256 0.0039	3.9	8.0	
0.0020	3.9	9.0	
0.00098	0.98	10.0	
0.00049	0.49	11.0	Clay
0.00024	0.24	12.0	
0.00012	0.12	13.0	
0.00006	0.06	14.0	

Macroscopic Core Descriptions

Igneous rocks are classified mainly on the basis of mineralogy and texture. When describing the cores, a checklist of macroscopic features was followed to maintain consistent and complete descriptions. One checklist for extrusive rocks and dikes is presented in Appendix B.

Two forms were used in the description of hard rocks - one for macroscopic description of cores and one for the description of thin sections. The data on these forms went directly into a computerized data base that is accessible to the entire scientific community.

Extrusives and Dikes

Basalts are termed aphyric, sparsely phyric, moderately phyric, or highly phyric, depending on the proportion of phenocrysts visible with the hand lens or binocular microscope (approximately × 10). Basalts are called (1) aphyric if phenocrysts clearly amount to < 1% of the rock, (2) sparsely phyric if phenocryst content ranges from 15%–25%, (3) moderately phyric at 2%–10%, and (4) highly phyric if phenocrysts amount to > 10% of the rock. Basalts are further classified by phenocryst type (e.g., a moderately plagioclase-olivine phyric basalt contains 2%–10% phenocrysts—most of them plagioclase, with some olivine).

Once the shipboard scientific party agreed on the lithologic description, the final core description was assembled on an igneous barrel sheet (Fig. 8). These barrel sheets are published in this volume. The procedure for describing the specimens is given in Appendix B.

Thin-Section Description

Thin-section billets of basement rocks recovered during Leg 119 were examined to help define unit boundaries indicated by hand-specimen core descriptions, to confirm the identity of the petrographic groups represented in the cores, and to define their secondary alteration mineralogy. At least one thin section was made of each unit identified from the hand specimen when sufficient rock was available. A number of dropstones were also studied in thin section.

In accordance with procedures generally adopted by petrologists during earlier DSDP/ODP legs, the petrographic units identified in thin section are described strictly by the presence of phenocryst assemblages or an individual phenocryst phase, but not by the relative abundance of phases as in the hand-specimen descriptions. Percentages of individual phenocryst phases were estimated visually and are reported on the detailed thin-section-description sheets (available in microform at the repositories). The terms *sparsely, moderately*, and *highly phyric* were used in the same manner as hand-specimen descriptions. When discrepancies arose over the composition and abundance of phenocryst phases between hand-specimen and thin-section analyses, thin-section descriptions were used in the lithostratigraphic summary.

Basement Alteration

Alteration effects resulting from seawater interaction with igneous rocks were described in hand specimens and thin sections. The width and color of any alteration halos around fractures or vugs were noted in the core descriptions.The identities of secondary minerals filling fractures, vesicles, and replacing igneous phases were estimated in core descriptions and refined in thin section, augmented in some cases onshore by X-ray-diffraction (XRD) and electron microprobe analyses made on shipboard thin sections. The total percentages of the various secondary minerals were also estimated from thin-section examinations.

BIOSTRATIGRAPHY

Leg 119 allows a unique opportunity to examine high-latitude microfossil faunas and floras from the Southern Hemisphere and to compare these faunas and floras with those at middle and low latitudes. The Leg 119 paleontologists established a biostratigraphic scheme for use during the cruise (Figs. 9 and 10). Both low-latitude microfossil zonations as well as zonal schemes established for the Southern Ocean were incorporated into this biostratigraphic framework. The scheme was established only as a reference to allow comparisons between the observed species and their stratigraphic ranges with a known chronostratigraphy. As such, it serves as a starting point in the iterative process of working toward a chronostratigraphy of the Southern Ocean.

The correlation of biostratigraphic zonations with the geomagnetic polarity time scale follows that of Berggren et al. (1985a, 1985b, 1985c) and is used here as the chronostrati-

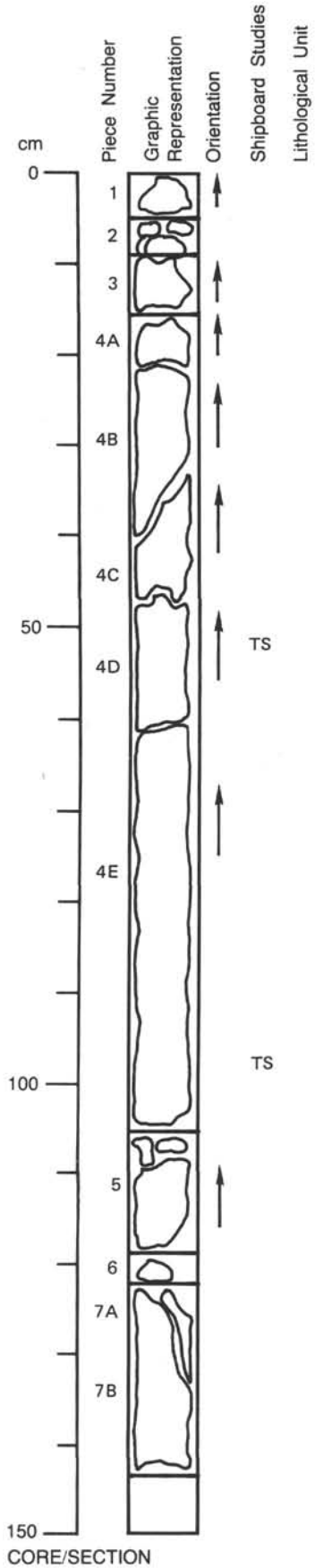

119-738C-33R-1

0-5 cm: **SPARSELY PLAGIOCLASE PHYRIC BASALT**

PIECE 1

CONTACTS: None
PHENOCRYSTS: Single crystals, uniform distribution
Plagioclase: 1-2%, 1-2 mm
GROUNDMASS: Fine grained
COLOR: Gray
VESICLES: 2%, round to oval, green rim, white neEdle-like zeolites
STRUCTURE: Massive
ALTERATION: Moderately
FRACTURES: 1 fracture at the bottom - filled by calcite, up to 3 mm thick, horizontal

5-37 cm: **VOLCANICLASTIC ROCK**

PIECES 2-4B

CONTACTS: Lower contact: slicken side, 55° dip
MATRIX: Fine grained, dull red, very highly altered
CLASTS: 0, 5-45 mm, rounded to angular, highly altered 60°-70° (?rotation?))
Type 1: Brownish black, vesicular (1-2 mm, 10-20%, ± regular distribution, dark green rim and small white zeolite needles & partially filled by calcite); (20-50%)
Type 2: Greenish gray; small irregular vesicles (mostly ≤ 0, 5 mm with green rim or filling regular distribution; 20%
FRACTURES: Few, mostly horizontal, filled by white calcite, 0, 5 mm 2, 5 wide, -2, 5 mm wide, irregular, cutting matrix and few clasts

37-135 cm: **VOLCANICLASTIC ROCK**

PIECES 4C-7A (INCL. 7B)

CONTACTS: Upper contact: fracture (filled with clasts of over and underlying rocks, embedded in calcitic matrix, 0-10 mm wide) and slicken slide, respectively; Lower contact: quite sharp, irregular
MATRIX: Fine grained, red, highly altered
CLASTS: Rounded to angular, 0, 5-35 mm, (40%
Type 1: Brownish black; vesicles (up to 5 mm long, partly totally filled by green to orange waxy mass; sharp straight contact; upper part filled by calcite; in 1 clast: in 2 vesicles horizontal contact; in 1 other clast contact dips 60°-70° (?rotation?))
Type 2: Greenish gray; small irregular vesicles (mostly ≤ 5 mm with green rim or filling, regular distribution); 20%
Type 3: Light grayish green; little vesicles (≤ 3%, dark green rim and white zeolite needles or totally filled by dark green substance; aphyric to sparsely feldspar phyric; moderately altered); distribution: mostly from 81-97 cm, not above, few in lower pat.
FRACTURES: Few horizontal and subvertical, irregular, 0, 5-1, 5 mm wide, some clasts rimmed by calcite, fractures cutting almost no clasts

135-143 cm: See 0-75 cm in Section 2

Figure 8. Igneous rock core description form.

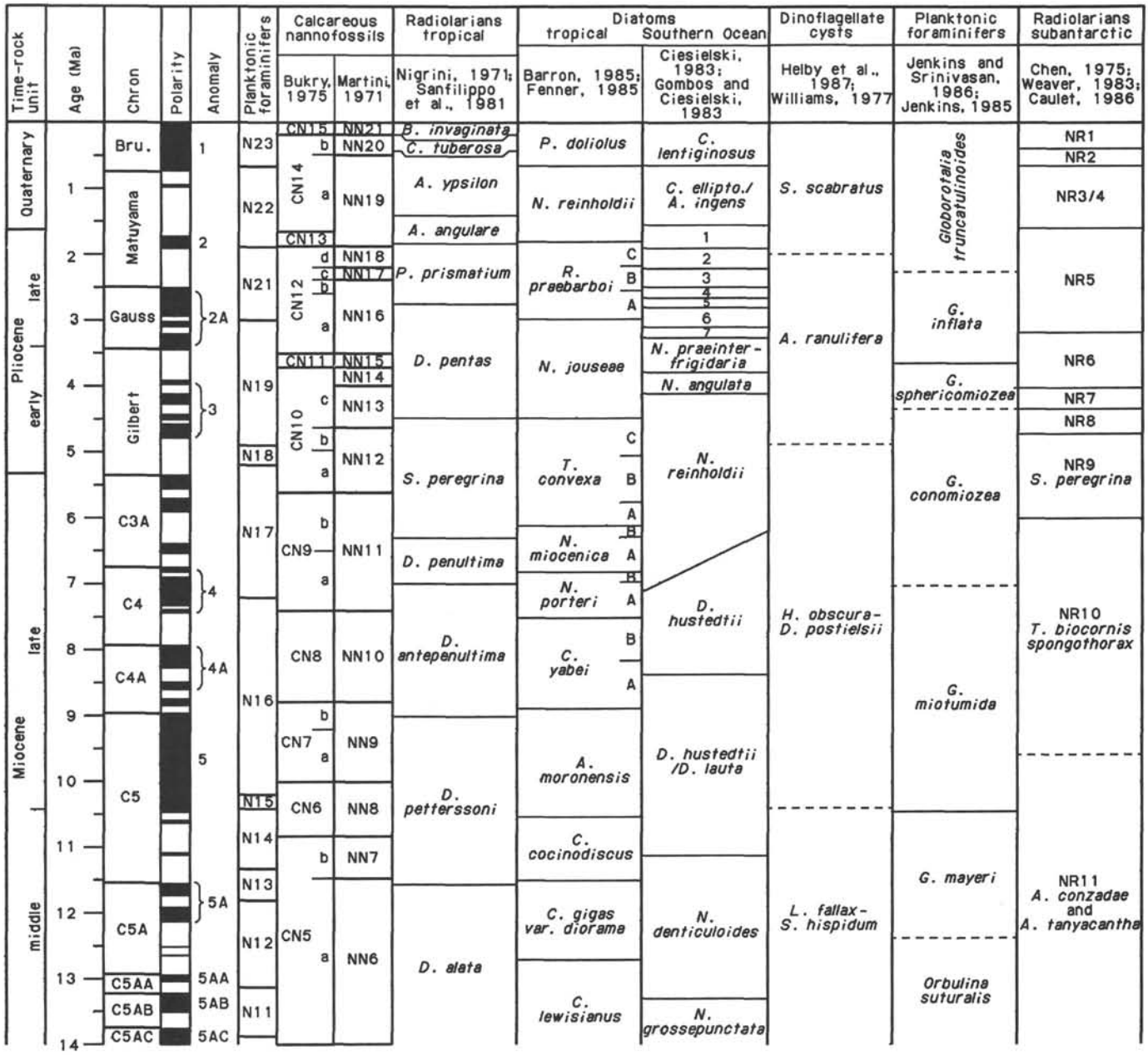

Figure 9. Biostratigraphic zonal scheme utilized for ODP Leg 119 studies for the upper Eocene to Quaternary with correlation to the geomagnetic polarity time scale of Berggren et al. (1985a, 1985b, 1985c). Zonal schemes are as follows: low-latitude planktonic foraminifers—Blow (1969) and Berggren (1969); low-latitude calcareous nannofossils—Bukry (1973, 1975), Okada and Bukry (1980), and Martini (1971); low-latitude radiolarians—Nigrini (1971) and Sanfilippo et al. (1981); low-latitude diatoms—Barron (1985) and Fenner (1985); Southern Ocean diatoms—Ciesielski (1983; modified, see text) and Gombos and Ciesielski (1983); dinoflagellate cysts—Helby et al. (1987) and Williams (1977); Southern Ocean mid-latitude planktonic foraminifers—Jenkins (1985) and Jenkins and Srinivasan (1986); and subantarctic radiolarians—Chen (1975), Weaver (1983), and Caulet (1986).

graphic framework for the Leg 119 studies. The epoch/stage boundaries used during Leg 119 studies are as follows:

	Age (Ma)
1. Pliocene/Pleistocene boundary	1.6
2. early/late Pliocene boundary	3.4
3. Miocene/Pliocene boundary	5.3
4. middle/late Miocene boundary	10.4
5. early/middle Miocene boundary	16.4
6. Oligocene/Miocene boundary	23.7
7. early/late Oligocene boundary	30.0
8. Eocene/Oligocene boundary	36.6
9. middle/late Eocene boundary	40.0
10. early/middle Eocene boundary	52.0
11. Paleocene/Eocene boundary	57.8
12. Cretaceous/Tertiary boundary	66.4
13. Campanian/Maestrichtian boundary	75.4
14. Santonian/Campanian boundary	80.4
15. Coniacian/Santonian boundary	88.0
16. Turonian/Coniacian boundary	89.0
17. Cenomanian/Turonian boundary	91.5

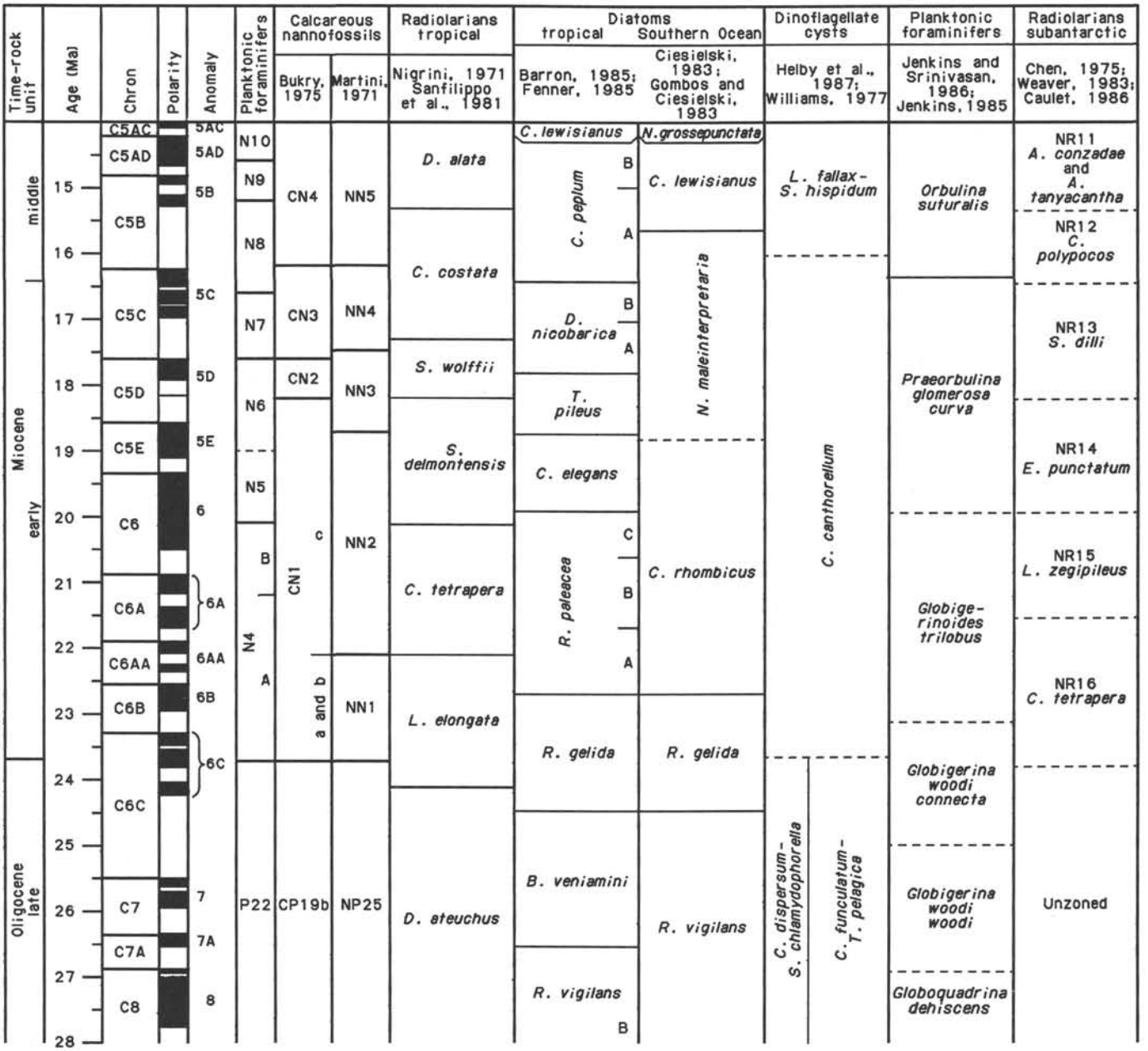

Figure 9 (continued).

The age estimates of Berggren et al. (1985a, 1985b, 1985c) for the normal magnetic polarity intervals are shown in Table 3. The microfossil zones and their calibration to the chronostratigraphy of Berggren et al. (1985a, 1985b, 1985c) are discussed in the following text.

Calcareous Nannofossils

The biostratigraphic zonations used in this report are those proposed by Martini (1971), Bukry (1973, 1975), and Roth (1978), complemented by the high-latitude zonation proposed by Wise (1983). All of the references are tied to the geomagnetic reversal time scale of Berggren et al. (1985a, 1985b, 1985c), as shown in Figures 9 and 10. For the late Mesozoic, the calibrations are based on interpolations of nannofossil events within magnetic chrons using sediment thicknesses in the Bottaccione section near Gubbio, as given by Monechi and Thierstein (1985). The estimated age of each calcareous nannofossil event, as used during Leg 119, is presented in Table 4.

Planktonic Foraminifers

Many important marker species used in standard low- to mid-latitude planktonic foraminifer zonal schemes are absent from the high southern latitudes, particularly within the Neogene. Development of new biostratigraphic zonations for the polar regions is in progress for the southern South Atlantic (ODP Legs 113 and 114), but these data are not available for the present study. These data are correlated with the Cenozoic planktonic zones of Blow (1979) using the FADs (first-appearance datums) and LADs (last-appearance datums) of important marker species that were recovered from the Leg 119 sites (Table 5).

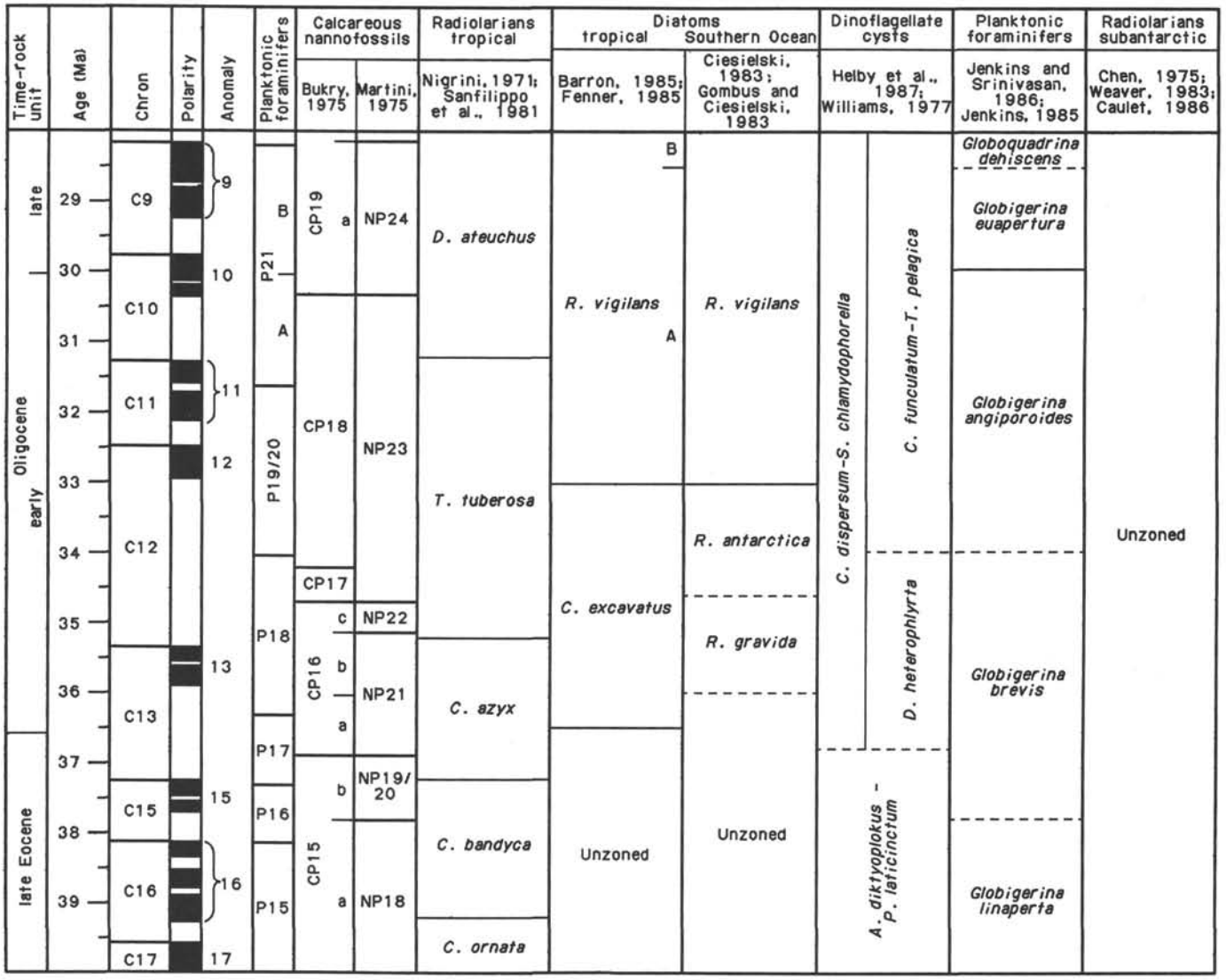

Figure 9 (continued).

Age assignments for these datums were determined based on the following:

1. Planktonic foraminiferal ranges defined by Toumarkine and Luterbacher (1985) for the Paleocene through Eocene.
2. Planktonic foraminiferal ranges defined by Bolli and Saunders (1985) for the Oligocene through Holocene.
3. Correlation with the magnetostratigraphic and geochronologic time scale of Berggren et al. (1985a, 1985b, 1985c). Some Cenozoic age determinations were also based on correlation with the southern, mid-latitude zonal scheme of Jenkins (1985).

The only low-latitude zonal marker recognized in Upper Cretaceous high-latitude sediments is *Abathomphalus mayaroensis* (B. T. Huber, pers. comm., 1988). Occurrence of this species enables correlation with the upper Maestrichtian *A. mayaroensis* Zone of Caron (1985). The pre-late Maestrichtian time interval is undifferentiated until results from southern South Atlantic Legs 113 and 114 are published.

Benthic Foraminifers

Bathyal benthic foraminifers provide no detailed biochronology. Their evolution is slow, and numerous taxa have ranges from the Eocene to the Holocene. In shallow water, a major faunal turnover is recognized at the end of the Cretaceous/Tertiary boundary (Huber, in press). In deep water, benthic assemblages changed near the Paleocene/Eocene boundary at the end of the Eocene and in the middle Miocene (e.g., Tjalsma and Lohmann, 1983; Miller and Katz, 1987; Douglas, 1973). The FADs and LADs of key species, however, do not always coincide in various studied deep-water basins (Thomas, 1985).

No benthic zonal scheme presently exists for the Antarctic region. The results of Leg 113 (Barker, Kennett, et al., 1988)

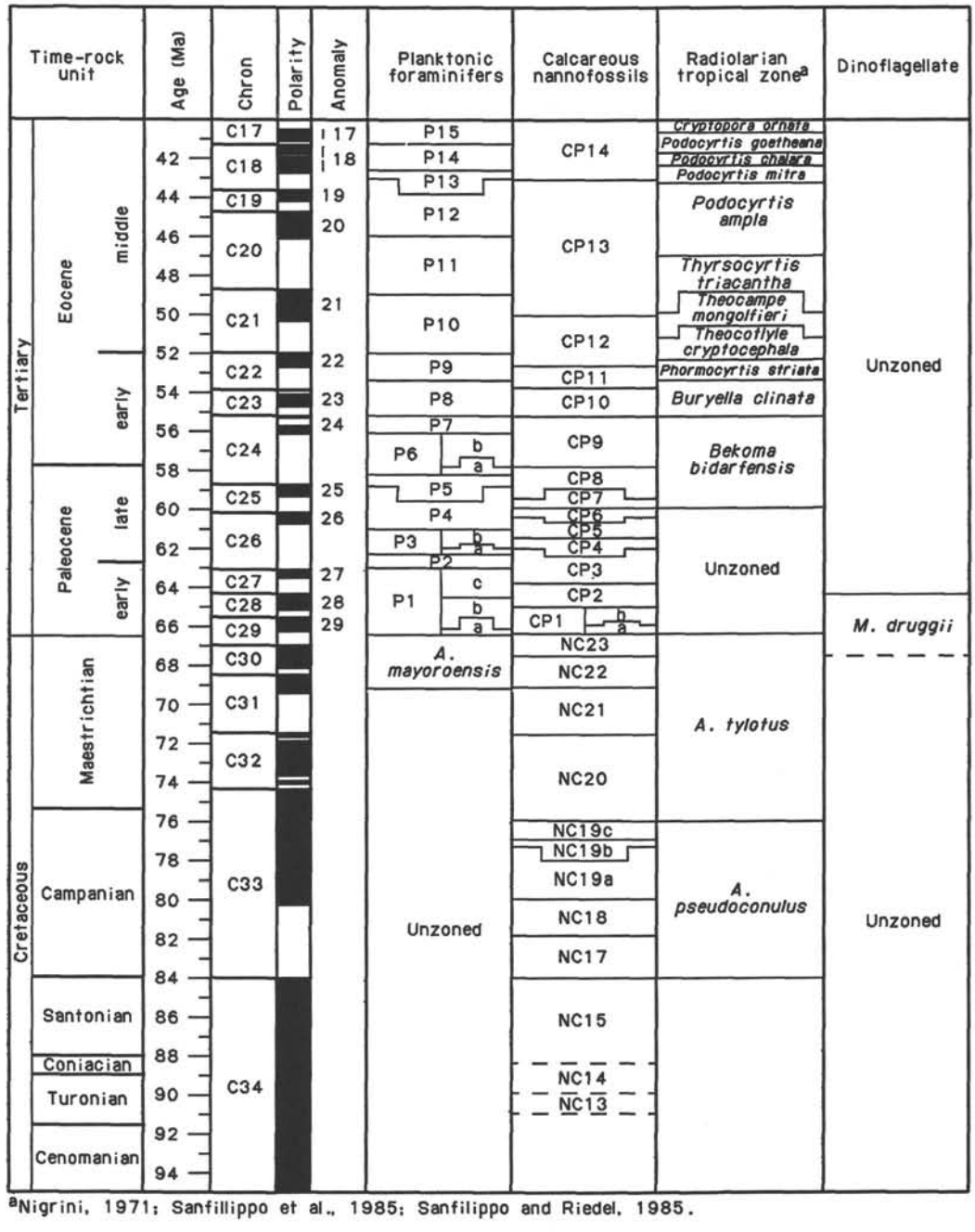

Figure 10. Biostratigraphic zonal scheme, correlation with the geomagnetic polarity time scale, and ages of the Paleogene nannofossils and foraminifer events are from Berggren et al. (1985a, 1985b). The ages of the Cretaceous nannofossil events are from correlation with the geomorphic polarity reversals in the Botteccione section (Monechi and Thierstein, 1985).

and Leg 120 will provide the most valuable data for comparison. For the Upper Cretaceous sediments, the benthic zonal scheme of Webb (1971) for the New Zealand Piripauan and Haumurian (middle Campanian–Maestrichtian) stages is most applicable, because the nominal agglutinated species have been recognized at the Lord Howe Rise (DSDP Site 208; Webb, 1973) and the Antarctic Peninsula (Huber, in press). Late Cenozoic benthic foraminifers of lower latitudes in the Indian Ocean (Ninetyeast Ridge) were described by Boltovskoy (1978).

Antarctic foraminifer assemblages were studied in the Ross Sea (DSDP Site 270) where four benthic faunal zones were recognized from the upper Oligocene to lower Miocene (Leckie and Webb, 1986).

Radiolarians

The Antarctic/Subantarctic radiolarian zonation, proposed by Chen (1975) and modified by Weaver (1983) and Caulet (1985, 1986), was used to zone Neogene sediments. No local detailed

Table 3. Revised geomagnetic polarity time scale for Cenozoic and Late Cretaceous time (after Berggren et al., 1985a, 1985b).

Normal polarity interval	Anomaly (Ma)	Normal polarity interval	Anomaly (Ma)
0.00–0.73	1	24.04–24.21	6C
0.91–0.98		25.50–25.60	7
1.66–1.88	2	25.67–25.97	7
2.47–2.92	2A	26.38–26.56	7A
2.99–3.08	2A	26.86–26.93	8
3.18–3.40	2A	27.01–27.74	8
3.88–3.97	3	28.15–28.74	9
4.10–4.24	3	28.80–29.21	9
4.40–4.47	3	29.73–30.03	10
4.57–4.77	3	30.09–30.33	10
5.35–5.53	3A	31.23–31.58	11
5.68–5.89	3A	31.64–32.06	11
6.37–6.50		32.46–32.90	12
6.70–6.78	4	35.29–35.47	13
6.85–7.28	4	35.54–35.87	13
7.35–7.41	4	37.24–37.46	15
7.90–8.21	4A	37.48–37.68	15
8.41–8.50	4A	38.10–38.34	16
8.71–8.80		38.50–38.79	16
8.92–10.42	5	38.83–39.24	16
10.54–10.59		39.53–40.43	17
11.03–11.09		40.50–40.70	17
11.55–11.73	5A	40.77–41.11	17
11.86–12.12	5A	41.29–41.73	18
12.46–12.49		41.80–42.23	18
12.58–12.62		42.30–42.73	18
12.83–13.01	5AA	43.60–44.06	19
13.20–13.46	5AB	44.66–46.17	20
13.69–14.08	5AC	48.75–50.34	21
14.20–14.66	5AD	51.95–52.62	22
14.87–14.96	5B	53.88–54.03	23
15.13–15.27	5B	54.09–54.70	23
16.22–16.52	5C	55.14–55.37	24
16.56–16.73	5C	55.66–56.14	24
16.80–16.98	5C	58.64–59.24	25
17.57–17.90	5D	60.21–60.75	26
18.12–18.14	5D	63.03–63.54	27
18.56–19.09	5E	64.29–65.12	28
19.35–20.45	6	65.50–66.17	29
20.88–21.16	6A	66.74–68.42	30
21.38–21.71	6A	68.52–69.40	31
21.90–22.06	6AA	71.37–71.65	32
22.25–22.35	6AA	71.91–73.55	32
22.57–22.97	6B	73.96–74.01	
23.27–23.44	6C	74.30–80.17	33
23.55–23.79	6C	84.00–118.00	34

biostratigraphic scales are proposed for the Paleogene and Cretaceous because (1) radiolarian zonations for the Oligocene, Eocene, Paleocene, and Cretaceous have not been established in high latitudes, and (2) most Cretaceous to Oligocene species identified on DSDP Legs 28 and 71 and collected by French researchers aboard *Marion Dufresne* are endemic to the Antarctic/Subantarctic area. Two tropical zones, proposed by Sanfilippo and Riedel (1985), have been tentatively used for the Late Cretaceous. They are defined as follows from the younger to the older:

1. *Amphipyndax tylotus* Zone (Foreman, 1977), presence of *A. tylotus*—Maestrichtian and upper Campanian.
2. *Amphipyndax pseudoconulus* Z. (Riedel and Sanfilippo, 1974, emend. Foreman, 1977, and the *A. enesseffi* Zone).
3. Presence of *A. pseudoconulus*—lower and middle Campanian.

Petrushevskaya (1975) pointed out some radiolarian events in the Eocene material of DSDP Leg 29, but she presented no zonations because Eocene radiolarians are rare in her samples.

Table 4. Estimated age and the magnetic calibration of the calcareous nannofossil events as used during Leg 119.

	Datum[a]	Age	Chron	Source
FO	*E. huxleyi*	0.275	C1 1N	Berggren et al., 1985c
LO	*P. lacunosa*	0.474	C1 1N	Berggren et al., 1985c
LO	*C. macintyrei*	1.45	C1 2R	Berggren et al., 1985c
FO	*G. oceanica*	1.68	C2 1N	Berggren et al., 1985c
LO	*D. brouweri*	1.9	C2 1R	Berggren et al., 1985c
LO	*D. variabilis*	2.9	C2A 1N	Berggren et al., 1985c
FO	*D. asymmetricus*	4.1	C3 1R	Berggren et al., 1985c
LO	*D. exilis*	8.85	C4A 3R	Berggren et al., 1985c
LO	*C. coalitus*	9.0	C5 1N	Berggren et al., 1985c
FO	*D. hamatus*	10.0	C5 1N	Berggren et al., 1985c
FO	*C. coalitus*	10.8	C5 2R	Berggren et al., 1985c
LO	*R. hesslandii*	11.5	C5 3R	[b]ODP Sites 689, 690
LO	*C. floridanus*	11.6	C5A 1N	Berggren et al., 1985c
FO	*R. perplexa*	13	C5AA N	[b]ODP Sites 689, 690
LO	*S. heteromorphus*	14.4	C5AD N	Berggren et al., 1985c
FO	*S. heteromorphus*	17.1	C5C 3R	Berggren et al., 1985c
LO	*S. belemnos*	17.4	C5C 3R	Berggren et al., 1985c
FO	*S. belemnos*	21.5	C6A 2N	Berggren et al., 1985c
LO	*R. bisecta*	23.7	C6C	Berggren et al., 1985c
LO	*R. scrippsae*	23.7	C6C	Berggren et al., 1985c
LO	*R. abisecta*	23.7	C6C	Berggren et al., 1985c
		23	C6 2N	[c]
LO	*Z. bijugatus*	24.6	C6 1R	Berggren et al., 1985a
LO	*R. bisecta*	25.4	C6 1R	
LO	*S. ciperoensis*	25.2	C6 1N	Berggren et al., 1985a
LO	*C. altus*	23.7	C6 2N	[b]
		27.4	C8 1N	[c]
LO	*S. distentus*	28.2	C9 1N	Berggren et al., 1985a
FO	*S. ciperoensis*	28.6	C9 1N	[c]
		30.2	C10 2N	Berggren et al., 1985a
FO	*S. distentus*	34.2	C12 1R	Berggren et al., 1985a
LO	*B. spinosus*	34.2	C12 1R	[c]
FO	*C. abisectus*	34.2	C12 1R	
LO	*R. umbilica*	34.6	C12 1R	Berggren et al., 1985a
LO	*B. serraculoides*	35.4	C12 1R	[c]
LO	*C. formosus*	35.1	C12 1R	Berggren et al., 1985a
		35.6	C13 2N	[c]
LO	*I. recurvus*	35.8	C13 2N	[c]
LO	*R. oamaruensis*	35.9	C13 2N	[b]
LO	*C. protoanulus*	36.7	C13 2N	DSDP Site 516
LO	*D. saipanensis*	36.7	C13 2R	Berggren et al., 1985a
FO	*C. altus*	36.7	C13 2R	[c]
FO	*C. floridanus*	36.7	C13 2R	
LO	*D. barbadiensis*	36.7	C13 2R	Berggren et al., 1985a
		37	C13 2R	[c]
FO	*R. oamaruensis*	37.2	C13 2R	ODP Sites 689 and 690
LO	*R. reticulofenestra*	37.4	C15 2N	
FO	*I. recurvus*	38.7	C15 2R	Berggren et al., 1985a
		39.6	C17 1N	[c]
FO	*C. oamaruensis*	39.8	C17 1N	Berggren et al., 1985a
FO	*H. situliformis*	39.9	C17 1N	[c]
LO	*C. grandis*	40	C17 1N	Berggren et al., 1985a
LO	*Necoccolithes dubius*	41.2	C17 3R	[c]
FO	*B. seraculoides*	42.4	C18 2N	[c]
LO	*C. solitus*	42.3	C18 3N	Berggren et al., 1985a
		43	C18 3R	DSDP Site 516
FO	*R. reticulata*	43.6	C19 1N	[c]
FO	*L. minutus*	43.8	C19 1N	
LO	*Nannotetrina fulgens*	45.4	C20 1N	Berggren et al., 1985a
LO	*C. gigas*	47.0	C20 1R	Berggren et al., 1985a
		45	C20 1N	[c]
FO	*R. umbilica*	44.8	C20 1N	
		46	C20 1N	Berggren et al., 1985a
FO	*C. gigas*	44.6	C19 1R	DSDP Site 516
FO	*Nannotetrina* sp.	50	C21 1N	
		49.8	C21 1N	Berggren et al., 1985a
LO	*D. sublodoensis*	52.6	C22 1N	Berggren et al., 1985a
LO	*T. orthostylus*	53.7	C22 1R	Berggren et al., 1985a
LO	*Fasciculithus*	57.6	C24 2R	Berggren et al., 1985a
FO	*D. multiradiatus*	59.2	C25 1R	Berggren et al., 1985a
FO	*D. nobilis*	59.4	C25 1R	Berggren et al., 1985a
FO	*H. riedeli*	60.0	C25 1R	Berggren et al., 1985a
FO	*D. mohleri*	60.4	C26 1N	Berggren et al., 1985a
LO	*C. danicus*	61.0	C26 1R	Berggren et al., 1985a
FO	*H. kleinpelli*	61.6	C26 1R	Berggren et al., 1985a
LO	*C. tenuis*	61.8	C26 1R	Berggren et al., 1985a
FO	*F. tympaniformis*	62.0	C26 1R	Berggren et al., 1985a

Table 4 (continued).

	Datum[a]	Age	Chron	Source
FO	*E. macellus*	63.8	C27 1R	Berggren et al., 1985a
FO	*C. tenuis*	65.9	C29 1N	Berggren et al., 1985a
FO	*C. primus*	66.1	C29 1R	Berggren et al., 1985a
FO	*P. sigmoides*	66.4	C29 1R	Berggren et al., 1985a
FO	*M. murus*	68.0	C30 1N	Monechi and Thierstein, 1985
FO	*N. frequens*	68.0	C30 1N	Monechi and Thierstein, 1985
FO	*L. quadratus*	69.3	C31 1N	Monechi and Thierstein, 1985
LO	*T. trifidus*	71.8	C32 1N	Monechi and Thierstein, 1985
FO	*T. trifidus*	76.0	C33 1N	Monechi and Thierstein, 1985
LO	*E. eximius*	77.0	C33 1N	Monechi and Thierstein, 1985
FO	*T. gothicus*	77.3	C33 1N	Monechi and Thierstein, 1985
FO	*C. aculeus*	79.9	C33 1N	Monechi and Thierstein, 1985
FO	*B. parca*	81.9	C33 1R	Monechi and Thierstein, 1985

[a] FO = first occurrence; LO = last occurrence.
[b] Unpublished data from Leg 113.
[c] Unpublished data from DSDP Site 516.

Table 5. Cenozoic foraminiferal datum events related to the Berggren et al. (1985b, 1985c) paleomagnetic time scale.

	Datum[a]	Chron[b]	Age (Ma)
FO	*Globorotalia truncatulinoides*	C2 1R	1.9
FO	*Globorotalia inflata*	C2A 2N	3.0
LO	*Globorotalia conomiozea*	C2A 2N	3.0
LO	*Globorotalia puncticulata*	C3 3N	4.4
FO	*Globorotalia conomiozea*	C3A 2R	6.1
LO	*Globorotalia zealandica*	C5C 3N	16.8
LO	*Catapsydrax dissimilis*	C5D 1N	17.6
FO	*Globorotalia praescitula*	C5D 1N	17.7
LO	*Chiloguembelina*	C10	30.0
LO	*Globigerina angiporoides*	C11	32.0
LO	*Globigerina ampliapertura*	C12	32.8
LO	*Pseudohastigerina*	C12/C13	34.0
LO	*Hantkenina*	C13	36.6
LO	*Globigerinatheka index*	C13	36.6
LO	*Acarinina*	C17	40.6
LO	*Truncorotaloides*	C17	40.6
LO	*Acarinina bullbrooki*	C18	43.0
FO	*Globigerinapsis index*	C21	45.0
FO	*Hantkenina*	C22	52.0
LO	*Planorotalites pseudomenardii*	C25	58.8
FO	*Planorotalites pseudomenardii*	C26	61.0
LO	*Subbotina pseudobulloides*	C26	61.7
LO	*Globoconusa daubjergensis*	C27	64.0
FO	*Planorotalites compressus*	C28	64.5
FO	*Subbotina pseudobulloides*	C29	66.1
FO	*Globoconusa daubjergensis*	C29	66.35
FO	*Eoglobigerina eugubina*	C29	66.35
LO	*Globotruncana*	C29	66.4
FO	*Abathomphalus mayaroensis*	C31	69.0
FO	*Globotruncana contusa*	C31	69.4
FO	*Globotruncna gansseri*		
LO	*Globotruncana calcarata*	C33	75.4
FO	*Globotruncana calcarata*	C33	76.0

[a] FO = first occurrence; LO = last occurrence.
[b] Paleomagnetic terminology after Tauxe et al. (1984).

Eocene age determinations are based tentatively on the occurrence of secondary marker species with ranges established in low-latitude regions (Sanfilippo et al., 1985). The estimated ages of the radiolarian events, as used during Leg 119, are presented in Table 6. For a detailed list of the zones, see Appendix C.

Diatoms

The diatom zonation of Ciesielski (1983) is used for the Neogene with the following modifications. The *Rocella gelida* Zone is that of Barron (1985) for low-latitude (i.e., the interval from the first occurrence of *R. gelida* to the first occurrence of *Rossiella* spp.). The overlying *Coscinodiscus rhombicus* Zone extends from the top of the *R. gelida* Zone to the first occurrence of *Nitzschia maleinterpretaria*. The *N. maleinterpretaria* Zone is taken as the range of the nominative species, whereas the immediately overlying *Coscinodiscus lewisianus* Zone extends to the first occurrence of *Denticulopsis hustedtii*, a datum which is more useful in the Southern Ocean than the last occurrence of *C. lewisianus* (R. Gersonde, pers. comm., 1988; J. Baldauf and J. Barron, unpubl. data). The *Nitzschia grossepunctata* Zone thereby becomes the interval from the first *D. hustedtii* to the last *N. grossepunctata*. The final modification to Ciesielski's (1983) zones involves the replacement of the last occurrence of *Denticulopsis dimorpha* as the marking datum for the top of the *D. hustedtii/D. lauta* Zone and the base of the overlying *D. hustedtii* Zone. The diatom zonation of Gombos and Ciesielski (1983) was used for the Oligocene (see Table 7 for a list of specific diatom events used during Leg 119). No older Paleogene diatoms were recovered during ODP Leg 119.

Table 6. Magnetic calibration and the estimated ages of radiolarian events as used during Leg 119.

	Datum[a]	Age (Ma)	Chron	Source
LO	*Stylatractus universus*	0.42	C1 1N	Morley and Shackleton, 1978
FO	*Cycladophora davisiana*	2.6	C2A 1N	Weaver, 1983
		2.8		
LO	*Prunopyle titan*	3.2	C2A 3N	Weaver, 1983
E	*Pseudocubus vema*	3.95	C3 1N	Weaver, 1983
FO	*Lamprocyrtis heteroporos*	3.95	C3 1N	Weaver, 1983
LO	*Triceraspyris coronata*	4.25	Gilbert	Weaver, 1983
FO	*Desmospyris spongiosa*	4.3	Gilbert	Weaver, 1983
LO	*Stichocorys peregrina*	4.4	Gilbert	Weaver, 1983
		4.6		
LO	*Didymocyrtis didymus*	5.4		Weaver, 1983
FO	*Stichocorys peregrina*	6.0		Weaver, 1983
LO	*Diartus hughesi*	8.6	9/10	Weaver, 1983
LO	*Actinomma tanyacantha*	9.5		Weaver, 1983
		9.8		
FO	*Theocalyptra bicornis*	9.5		
	spongothorax	9.8		Weaver, 1983
LO	*Cyrtocapsella japonica*	10.5		
		11.2		Weaver, 1983

[a] FO = first occurrence; LO = last occurrence; E = evolutionary transition.

Dinoflagellates

The dinoflagellate cyst zonation referred to in the text is that of Helby et al. (1987), which is based on the Mesozoic of Australia. That part of the scheme relevant to the present study is as follows:

Manumiella druggii Interval Zone
Base: oldest occurrence of *Manumiella druggii*
Top: oldest consistent, abundant occurrence of *Trithyrodinium evittii*
Significant accessory forms: *Manumiella seclandica, Manumiella conorata plexus*, and *Alisocysta circumtabulata*.

Other dinoflagellate cyst ranges not referable to the above zoned scheme are based on the worldwide biostratigraphic summaries written by Williams and Bujak (1985).

Methods

Calcareous Nannofossils

The relative abundance of calcareous nannofossils in the fine fractions of each sample studied is given in the biostratigraphic

Table 7. Southern Ocean diatom datums.

Datum[a]	Age (Ma)	Chron	Reference
LO abundant *H. karstenii*	0.195	C1 1N	Burckle et al., 1978
LO *A. ingens*	0.62	C1 1N	Ciesielski, 1983
LO *C. elliptopora*	0.65	C1 1N	Ciesielski, 1983
LO *R. barboi*	1.58	C1 2R	Ciesielski, 1983
LO *C. kolbei*	1.89	C2 1N	Ciesielski, 1983
FO *C. elliptopora*	2.2	—	Ciesielski, 1983
LO *C. vulnificus*	2.22	C2 1R	Weaver and Gombos, 1981
FO *A. actinochilus*	2.3	—	
LO *C. insignis*	2.49	C2A 1N	McCollum, 1975; Ciesielski, 1983
LO *N. weaveri*	2.64	—	Ciesielski, 1983
LO *N. interfrigidaria*	2.8	C2A 1N	Ciesielski, 1983
FO *C. vulnificus*	3.1	—	Ciesielski, 1983
FO *N. interfrigidaria*	3.7–3.8	C3 1R	R. Gersonde (pers. comm., 1988)
FO *N. "angulata"*	4.2	C3A 2N	Ciesielski, 1983
LO *D. hustedtii*	4.5	C3A 4R	Ciesielski, 1983
FO *T. gracilis*	4.8	—	McCollum, 1975
LO *T. miocenica*	5.1	C3 5R	Burckle, 1978
LO *T. praeconvexa*	5.8	C3A 2N	Burckle, 1978
FO *T. miocenica*	6.1	C3A 2R	Burckle, 1978
LO common *D. hustedtii*	6.2	C3A 2R	(61°S, Leg 119)
LO common *D. hustedtii*	7.0	C4 2N	(50°S, Leg 119)
FO *N. cylindrica*	7.3	C4 2N	(Leg 119)
LO *D. dimorpha*	8.4–8.5	C4A 2N	(Leg 119)
LO common *D. dimorpha*	10.0	C5 1N	R. Gersonde (pers. comm., 1988)
LO *D. praedimorpha*	10.5	C5 1R	Ciesielski, 1983
LO *N. denticuloides*	11.0–11.1	C5 R	R. Gersonde (pers. comm., 1988)
FO *D. dimorpha*	11.1–11.2	C5 R	R. Gersonde (pers. comm., 1988)
LO *C. nicobarica*	12.2		Barron, 1985
FO *D. praedimorpha*	12.8–12.9	C5AA N	R. Gersonde (pers. comm., 1988)
FO *N. denticuloides*	13.5	C5AB N	R. Gersonde (pers. comm., 1988)
LO *N. grossepunctata*	13.8	—	R. Gersonde (pers. comm., 1988)
FO common *D. hustedtii*	13.8	—	Barron, 1985
FO *D. hustedtii*	14.2	—	R. Gersonde (pers. comm., 1988)
FO *N. grossepunctata*	15.0–15.1	C5B R	R. Gersonde (pers. comm., 1988)
LO *N. maleinterpretaria*	15.6	—	Barron, 1985
FO *D. nicobarica*	17.8	C5D N	Barron, 1985
FO *N. maleinterpretatia*	18.8	C5E N	Barron, 1985
FO *R. gelida*	24.5	—	Barron, 1985

[a] FO = first occurrence; LO = last occurrence.

summary tables of each site and near the left-hand margin of the range charts. In addition, the relative abundances of individual taxa within the nannofossil assemblages are documented in the range charts of each site. These visual relative abundances estimates are given a letter code with the following meaning:

A = abundant (>10%)
C = common (1%–10%)
F = few (0.1%–1%)
R = rare (<0.1%)

Preservational observations follow the schemes of Roth and Thierstein (1972) and Roth (1973) and separate between etching (caused by dissolution before or after sedimentation) and diagenetic overgrowth on a scale of none (blank), slight (1), moderate (2), and strong (3).

Foraminifers

Abundance of foraminifers is based on visual estimates of the >63-μm-size fraction in several fields of view. In cases where siliceous microfossils and fine detritus compose the finer size fraction, a 150-μm sieve was used to separate the foraminifer-rich coarse residue. The small fraction, however, was studied for small-sized taxa. In rich samples abundance estimates are difficult. The scale of abundance is as follows:

A = abundant (>40%)
C = common (15%–40%)
F = few (1%–15%)
R = rare (<1%)

The same scheme is used to express the abundance of particular species as percent of total population. The degree of preservation is estimated as follows:

G = good (no evidence of surface abrasion or dissolution)
M = moderate (dissolution, calcite overgrowth, or fragmentation common but minor)
P = poor (tests highly fragmented; identification difficult)

Samples of 20 cm^3 were washed through 63- and 150-μm sieves, dried on a hot plate, and picked for foraminifers and other microfossil constituents. Somewhat consolidated samples were first processed in hydrogen peroxide (H_2O_2, 10%) before being washed and dried. All mud-line samples are preserved with formaldehyde and stained with Rose Bengal.

Radiolarians

Abundance

Radiolarians are "abundant" when they constitute 5% or more of the total sediment, "common" when they compose from 1% to 5% of the sediment, and "rare" when in traces. Abundance estimates on radiolarian slides are not realistic because radiolarian skeletons were concentrated after processing. But they were considered "abundant" when two drops of the

preparation were sufficient to set at least 1000 specimens on a slide, "common" when the number of specimens decreased to between 100 and 1000, and "rare" when less than 100 debris were seen.

Preservation

Preservation is "good" when 75% of the population can be determined to the species level, "moderate" when 50% to 75% of the debris can be recognized, and "poor" when only 25% of the debris are determined to the species level.

Reworking

Degree of reworking was estimated in the percentage of specimens unquestionably older than the main assemblage.

Diatoms

For intervals enriched with biogenic silica, only nonprocessed, strewn slides were examined. Otherwise, each sample (about 5 cm^3 of sediment) was processed in a beaker using hydrogen peroxide (H_2O_2) and hydrochloric acid (HCl) and heated to speed the chemical reaction. Upon completion of the reaction, the beaker was filled with distilled water. After 1.5 hr, the water was decanted, and the beaker was refilled with distilled water. This procedure was repeated until a pH of about 6 was achieved. A few drops of residue were mounted between slides using Hyrax mounting medium. The strewn slides were examined at a magnification of 700×, and species identification was verified at a magnification of 1250×.

Strewn slides were examined using a Zeiss compound microscope. At least 450 fields of view (0.5 mm in diameter) were examined. Species were considered abundant when two or more were present in one field of view at 500×, common if one species was encountered in two fields of view, few if one specimen was observed in one horizontal traverse, and rare if less than one per traverse. Criteria for distinguishing whole from partial diatoms follow Schrader and Gersonde (1978).

Preservation was considered good if more than 95% of the diatoms were whole and valves show virtually no partial dissolution, reprecipitation, or fracturing. Moderate preservation consisted of 30% to 95% whole valves, with moderate breakage and slight dissolution and some fragile species still complete. In addition, girdle bands were generally intact. If less than 30% of the diatoms were whole, preservation was regarded as poor. Most diatoms show extensive breakage, partial dissolution, and pitting. Delicate structures were generally not preserved, and fragile species and girdle bands were generally not intact. If no diatoms were found, the sample was recorded as barren.

In addition to standard procedures for biostratigraphic analysis, plankton samples were collected in order to compare the diatoms in the phytoplankton with those in the sediment. Mud samples and samples in the first 30 m of downhole section were taken and processed according to Baldauf (1984). After completion of the first site, the scientific party on the *Maersk Master* took living phytoplankton samples daily in a time series from 35 near-surface tows (5-m net). These samples were fixed with glutyraldehyde and observed in rinsed and cleaned permanent mounts, following the methods of Fryxell (1975) and based on the assumption that net plankton are more likely than nannoplankton to sink out of the water column into the sediments instead of being advected until dissolved. Also, net plankton are less ubiquitous than nannoplankton and can aid paleoecological interpretation.

Percent frequency in each living sample based on counts of 300 valves together with percent frequency averaged over the total-time series were used for comparison with the frequency of diatoms in the sedimentary samples. We tried to distinguish between life stages and relationship to ice cover.

Additional samples and oceanographic information recovered from the upper 200 m of the water column include (1) filtered water samples for nannoplankton, (2) opening and closing vertical-net hauls to integrate over discrete layers, temperature, and salinity, (3) Secchi disc readings, and (4) short-term sediment trap deployments as service demands allowed. In this way, we will be able to assess the stability of the upper water column in the drill area and the short-term fluxes to the sediments. We will also be able to perform quantitative estimation of changes in abundance in the open ocean over short time scales.

Dinoflagellates

Palynology processing techniques for Leg 119 involved dissolving a 10-cm^3 sample in 10% HCl. Fresh acid was continuously added, allowing sediment to settle, and the material was decanted until all reaction ceased. The sample was allowed to settle, the liquid was decanted, and water was added. The previous step was repeated until the sample was neutral when tested with litmus paper. At this stage, we proceeded to methods A or B.

Method A

In method A, we gently washed the sample through a 38-μm metal sieve using a fine water spray. Then the remaining residue was collected in a clean pipette. A drop of the residue was placed on a glass slide and examined under the microscope. If the sample did not contain too much mineral matter, we proceeded to the slide preparation. If the sample contained a high proportion of mineral matter, some of it was removed by swirling the residue on a large watch glass and removing the finer material with a pipette.

Method B

The sample was placed in the aspirator funnel containing a sheet of nylon mesh. We aspirated and vacuumed the sample until the finer material was removed and then collected the residue in a pipette. Again, as in method A, we checked a drop of residue for mineral matter and either proceeded to slide preparation or swirled the sample to obtain finer material for slide preparation.

Slide Preparation

Glycerin jelly was placed in a test tube. The test tube was put in a beaker of warm water and left on a warm hot plate. When the jelly was liquefied, we used a pipette to place one or two drops on a clean glass slide and added one or two drops of the sample residue. This combination was mixed well before a coverslip was carefully placed on the slide and put on the warm hot plate to allow the material to spread. After the material was removed from the hot plate and allowed to set, it was labeled and examined.

PALEOMAGNETICS

Procedures

The majority of core material retrieved during Leg 119 consisted of sediments. We used cubic sampling boxes (Perspex plastic sample cubes—6 cm^3 in volume) to sample poorly lithified sediments throughout the cores. The sediment cores were oriented by scribing vertical orientation marks on the split-core surface, parallel to the core axis. The sample cubes were oriented relative to the orientation line and pressed into the sediments. The sample was removed with a stainless-steel spatula, and caps sealed the sampling cubes.

We sampled each core section at intervals of approximately 50 cm. We were careful to avoid drilling disturbance; thus, the sampling interval varied, reflecting the lithology and nature of the sediments. In order to avoid sediments containing glacially

derived erratics, sampling was restricted to fine-grained lithologies in general.

We found lithified sediments in the deeper portions of the holes. In order to sample these rocks, core segments were oriented and removed from the core liner; then a rock saw was used to cut cubic samples, which were placed in Perspex sample cubes and sealed. We cut 1-in- (2.5-cm-) diameter cylinders in some lithified core sections.

Measurements of the natural remanent magnetization (NRM) were made aboard ship using a MOLESPIN magnetometer. We used alternating field demagnetization on selected samples to evaluate the magnetic stability for representative samples.

The shipboard cryogenic magnetometer was not available at the beginning of the cruise because of delays in the shipment and delivery of liquid helium. Helium was transferred at sea from the *Maersk Master* to the *JOIDES Resolution*, and the cryogenic magnetometer was filled with liquid helium while underway. During this initial filling, a strong magnetic field (in excess of 5000 nT) was trapped in the machine. Unfortunately, we took measurements from Sites 737 and 738 while the cryogenic retained this high trapped field (and while substantial problems existed with the cryogenic magnetometer computer system).

After Site 738, we thermally cycled the cryogenic magnetometer, and a much smaller field of 400 nT was trapped within the cryogenic magnetometer. We took subsequent measurements at this much lower, trapped-field level.

Several problems in the cryogenic magnetometer computer software were identified during Leg 119, primarily involving the incorrect coupling of background noise levels on the three magnetometer axes with measurements on other axes. The background noise measurements (from the incorrect axes) were often larger than the observed magnetic measurements. In most cases, this resulted in nearly uniform values calculated for declination and inclination (most inclinations falling near 45°). When we coupled the correct background noise measurements with the correct magnetic measurements, the magnetic inclinations steepened, as would be expected for high-latitude sites, and the declinations in unoriented cores varied, as would be expected. The computer-program problem is significant because the program has been on the cryogenic system since it was delivered to the ship. Thus, all prior legs have been affected.

A second significant problem is that the cryogenic system does not always correctly register flux jumps. The flux jumps were not recorded as part of the computer program; therefore, the measurements from Hole 737B and Site 738 could not be corrected after the problems were discovered.

A third problem involved records of spurious results. Measurements exceeding the sensing range of the cryogenic magnetometer were often recorded, but the source of this problem could not be identified while at sea.

After we resolved the major problems, we measured the archive halves of the core sections with the cryogenic magnetometer, taking a 10-cm section of the core made at 10-cm intervals down the core. The NRM was measured for all core sections. We used the corrected computer program for measurements from all sites after Site 738.

The reversal stratigraphy observed within the cores recovered during Leg 119 was correlated with biostratigraphic zonations. These zonations were determined by shipboard scientists using calcareous nannofossils, foraminifers, diatoms, radiolarians, and dinoflagellates. We correlated the resulting reversal stratigraphy to the time scale of Berggren et al. (1985b, 1985c).

Bulk Magnetic Susceptibility

Whole-core bulk-susceptibility measurements were made on core sections of Holes 736A, 738B, 738C, 744A, 744B, 744C and 745B. Split-core measurements of susceptibility were made on the archive halves of core sections from Holes 736B and 736C. We took measurements using a Bartington magnetic-susceptibility meter interfaced with the shipboard PRO-350 computer.

The measurements are pass-through measurements taken at 2-cm intervals, not discrete sample measurements. The pass-through measurements average the bulk susceptibility over several centimeters of core. For the purpose of bulk-susceptibility measurements, the cores were exposed to a 1-Oe alternating field. The susceptibility meter measures volume susceptibility (K), which is reported in cgs units. Shore-based laboratory measurements of discrete samples from Sites 738 and 745 confirm measurements made at the lower-scale range on the shipboard equipment.

ORGANIC GEOCHEMISTRY

The organic geochemistry program for Leg 119 included (1) analyses of hydrocarbon gases, (2) determination of total carbon, inorganic carbon, and organic carbon, and (3) characterization of the organic matter by Rock-Eval pyrolysis. We monitored gases every third core (about 30 m) by headspace, and wherever a gas pocket occurred, by vacutainer. Generally, we performed the analyses on every third core according to ODP protocol (Emeis and Kvenvolden, 1986; Kvenvolden and McDonald, 1986), with more frequent analyses to meet safety and site objectives. For example, more frequent gas analyses were done when the C_1/C_{2+} ratio approached 1000, and Rock-Eval analyses were done on sequences with a high organic content (as determined by dark color or by a petroleum smell).

Hydrocarbon Gases

We extracted gas from samples using a headspace technique modified after Bernard et al. (1978) and Kvenvolden and Redden (1980). In this procedure, a weighed sample (approximately 5 cm^3) was sealed in a 22-mL glass vial with septum, purged with helium, and heated at 70°C to partition the gases into the helium headspace. We analyzed the headspace gases using a Hewlett-Packard (HP)-820 natural gas analyzer on a HP-5890A gas chromatograph with a flame-ionization detector (FID) and a thermal-conductivity detector (TCD). The sample was introduced through a 0.25-mL sample loop. The HP measured hydrocarbon gases to C_6. The headspace sample was also analyzed on a Carle AGC Series 1000/Model 211. The Carle only analyzed methane (C_1), ethane (C_2), and propane (C_3), but was much quicker than analysis with the three-column HP system. The headspace sample was sampled as soon as possible so that minimal volatiles were lost.

An alternative headspace technique described by Kvenvolden and McDonald (1986) involved adding a 5-cm whole-round section of the core with 100-mL He-purged water to a 1-pt can (previously prepared with two septa). The headspace was purged with He after the can was sealed. After shaking vigorously for 10 min, a sample of the headspace was analyzed as with the small vial analysis.

When we observed gas pockets separating the core within the core liner, we used the vacutainer method, in which an evacuated can with a needle attached punctured the core liner where gas physically separated the sediments. This gas was analyzed with the HP and Carle systems described previously.

Carbon Analysis

Shipboard total carbon was analyzed using a Coulometrics 5020 Total Carbon Apparatus coupled with the 5010 CO_2 Coulometer. Freeze-dried sediment was weighed into a platinum boat and put into a combustion furnace at 990°C. This technique involves oxygen passed through a barium-chromate combustion catalyst/scrubber that flows through the system to oxidize carbon and serve as a carrier gas. The liberated CO_2 passes through

traps to remove noncarbon-combustion products (SO_2, SO_3, NO_X, and others). The gas then passes into the coulometer cell, which consists of an aqueous solution containing a colorimetric indicator and monoethanolamine. The CO_2 is quantitatively absorbed by reacting with monoethanolamine to form hydroxethylcarbamic acid. The acid makes the transmittance (%T) increase, which is monitored by a photodetector. As %T increases, titration current stoichiometrically generates base at a rate proportional to %T. The current stops as the solution returns to its original color. Titration current is continuously monitored and integrator calculated for the percentage of carbon in the sample.

Inorganic (carbonate) carbon was determined using a Coulometrics 5030 Carbonate Apparatus also coupled with a 5010 Coulometer. A freeze-dried sample of known weight was acidified in a heated reaction vessel. Carbon dioxide-free air (scrubbed with KOH) carries the CO_2 through a $AgNO_3$ solution to remove unwanted gases evolved from the acidification. The CO_2 is then passed into the coulometer cell described previously.

Total organic carbon was calculated as the difference between total carbon and inorganic carbon when both were determined. Aliquots from one homogeneous sample were analyzed for both total carbon and inorganic carbon. (In some instances it is easier to present inorganic carbon as carbonate carbon. This is done by multiplying the percentage of inorganic carbon by 8.33.)

Rock-Eval Pyrolysis

Rock-Eval pyrolysis characterizes the amount, source, and maturity of the organic matter present. About 100 mg of ground, dried sediment was heated from 250° to 550°C at a rate of 25°C/min. The resultant gases were sent through a TCD and FID to monitor CO_2 and hydrocarbons, respectively. The four following parameters characterize the organic matter for each sample (Tissot and Welte, 1984):

1. S1: free-hydrocarbon fraction of organic matter.
2. S2: quantity of hydrocarbons released by pyrolysis of kerogen up to 550°C.
3. S3: corresponds to CO_2 released from pyrolysis of kerogen (from 250° and 390°C to avoid CO_2 from carbonate) and measures oxygen amount in the kerogen matrix.
4. T_{max}: top of S2 peak related to maturity of kerogen.

Generally, total organic carbon (TOC) is measured on the Rock Eval; however, TOC measurements on this Rock Eval have never been reliable (Kvenvolden and McDonald, 1986). When organic material from several sources is present, multiple S2 peaks can result. This can also affect the T_{max}. Admixtures of carbon that vary in maturity can result in a high T_{max} even if the majority of carbon is immature because T_{max} is taken as the highest temperature of S2 hydrocarbon evolution.

Four parameters can also be calculated from the four measured parameters and TOC. Hydrocarbon index (HI) is 100 (S2)/TOC (expressed as mg hydrocarbons/g rock). Oxygen index (OI) is 100 (S3)/TOC (expressed as mg CO_2/g rock). Productivity index (PI) is defined as the S1/(S1 + S2) ratio. PI generally tells the relative amount of hydrocarbons in the zone. Petroleum potential (PC) is 0.08(S1 + S2). PC is the pyrolysized carbon and represents the maximum amount of hydrocarbon that could be produced under ideal conditions. Both PI and PC are expressed as mg hydrocarbons/g rock. Guidelines for interpretation of these data can be found in Tissot and Welte (1984) and Kvenvolden and McDonald (1986).

INORGANIC GEOCHEMISTRY

Two shipboard, interstitial-water sampling programs were carried out during Leg 119. During the first program, we obtained a 5- to 10-cm whole-round minicore from every third core (about 30 m) for routine interstitial-water analyses. Sediment minicores were obtained as soon after core retrieval as possible and were squeezed at room temperature for interstitial waters using a stainless-steel press (Manheim and Sayles, 1974). Water was squeezed from the sediments at a maximum pressure of 45,000 psi, collected in plastic syringes, and filtered through prewashed millipore filters with a nominal pore diameter of 0.45 μm. Subsequent to filtration, a 5-mL aliquot of each interstitial-water sample from the routine sampling program was analyzed for total dissolved solids (salinity), pH, alkalinity, calcium, magnesium, chlorinity, sulfate, silica, ammonium, and phosphate using the methods outlined below.

All aliquots were stored in a refrigerator when analyses were not in progress. The remainder of each interstitial-water sample was flame-sealed in plastic tubes and glass ampoules for postcruise analyses.

A second high-resolution, interstitial-water sampling program was introduced during Leg 119 to collect interstitial-water samples every few meters in order to identify zones where active silica diagenesis reactions were affecting the dissolved silicon profile. The sample size was 10 cm^3 rather than the normal whole-round sample volume of around 300 cm^3. The high-resolution method could still be used in deeper sections, where interstitial-water samples could not be recovered by the normal squeezing method. In addition, these samples were stored under cold, inert atmospheric conditions to minimize temperature and oxidation effects.

The 10-cm^3 sediment samples were collected at approximately 3-m intervals at all Kerguelen Plateau sites and at the first Prydz Bay site (739). They were stored in sealed bags at 4°C. Within 12 hr of splitting, each sediment sample was transferred to a 50-mL centrifuge tube, which was flushed with He and stored at 4°C.

Within 48 hr of splitting, interstitial waters from the high-resolution samples were recovered using the following method. Five cm^3 of total dissolved solids (salinity) were measured using an AO Scientific Instruments optical refractometer. Calcium, magnesium, and chloride concentrations were determined by wet chemical titrations described by Gieskes (1974) and modified by Gieskes and Peretsman (1986). Sulfate concentrations were measured with a Dionex ion chromatograph (Gieskes and Peretsman, 1986). Silica, ammonium, and phosphate concentrations were measured by colorimetric methods using a Bausch and Lomb Spectronic 1001 spectrophotometer (Mann and Gieskes, 1975; Gieskes and Peretsman, 1986). IAPSO (International Association of Physical Sciences Organizations) standard seawater was the primary standard for all shipboard analyses. For a detailed description of all shipboard analytical techniques see Gieskes and Peretsman (1986).

BIOLOGY AND OCEANOGRAPHY

The ice picket vessel *Maersk Master* accompanied *JOIDES Resolution* on Leg 119 to permit drilling operations near drifting ice. When ice conditions were favorable, permission was given for the escort vessel to move a few kilometers from the drill ship to conduct scientific operations. These operations included deploying and recovering sediment trap arrays (see Biggs et al., this volume); measuring temperature, salinity, and light penetration; conducting phytoplankton net tows; and taking water samples. Bucket samples were also collected every 2 hr while in transit.

Methodology

Water-Column Profiling

A SEACAT SBE 19 conductivity, temperature, and depth recorder (Sea-Bird Electronics) provided water-column profiles from 0 to 200 m. These data were recorded internally and later

transferred to a computer for storage and manipulation. The profiles were taken before the water casts so that the water collection bottles could be placed at desired depths in relation to the mixed layer.

Light Penetration

Estimates of light extinction coefficients and light penetration (i.e., represented as percent of total incident irradiation) were made using a 30-cm Secchi disc (Evans et al., 1987). By raising and lowering the Secchi, the exact depths were determined using the following formula:

Sampling depth in meters = (ln %light-depth/100) × (Secchi depth in meters/ − 1.7)

Phytoplankton Net Tows

Phytoplankton samples were routinely collected by pulling nets of various sized meshes (i.e., 35, 64, and 80 μm) for different target populations through the water column. During this sampling period, three procedures were used: (1) stratified vertical net hauls using opening and closing nets, (2) horizontal surface-net tows, and (3) vertical net hauls with standard phytoplankton nets.

Water Collection

Water was collected from various depths down to 200 m below sea level using a set of 5-L Niskin water-sampling bottles. A Niskin bottle is a PVC cylinder with caps on each end that are fastened to the cylinder by a strong elastic band through the center of the cylinder. A triggering mechanism mounted on the side of the bottle held the end caps in the open position until they were released by the action of a heavy metal messenger that slid down the wire on which the bottles were lowered. A messenger hung beneath each bottle was released when the bottle closed and slid down the wire to trigger the next bottle. In this manner water samples were collected from any depth desired. Water was drawn off through a valve in the side of each bottle.

Surface-water samples were collected while on station and underway using a bucket. Surface temperature was measured using a bucket thermometer; surface salinity was measured with a hand refractometer.

Sample Processing

Net Samples

Material from horizontal net tows and vertical net hauls was preserved in 125-mL aliquots with 1%–2% glutaraldehyde. These concentrated samples provided abundant material for species identification. A preliminary species list included in Table 8 was compiled for each site through examination of the material collected by these phytoplankton net tows. In addition, live material was examined and photographed using both bright field and phase contrast, with epifluorescence microscopy used to observe active chlorophyll in living, healthy cells. Relative abundance data will be assessed from the stratified net hauls. Samples were processed as in Baldauf (1984) and Fryxell (1975).

Water Samples

The wide variety of analyses performed on the water samples collected with the Niskin bottles and buckets is described briefly in the following.

In order to measure chlorophyll concentrations using the fluorescence method (Holm-Hansen et al., 1965; Jacobsen, 1982; Loftus and Carpenter, 1971), 1 L of seawater from each Niskin bottle and surface bucket sample was filtered onto Whatman GF/F filters (pore size 0.7 μm). Pigments were extracted for 48 hr in darkness at a temperature of −20°C using a 90% acetone solution. A Turner 110 fluorometer was used to measure the fluorescence of chlorophyll and phaeopigments.

Table 8. Phytoplankton species list of ODP Leg 119.

Diatoms

Actinocyclus actinochilus (Ehrenberg) Simonsen
Actinocyclus ehrenbergii Ralfs *in* Pritchard
Actinocyclus ingens Rattray
Actinocyclus octonarius (Ehrenberg) Ehrenberg
Actinocyclus spiritus Watkins
Amphiprora sp.
Asteromphalus hookeri Ehrenberg
Asteromphalus hyalinus Karsten
Asteromphalus parvulus Karsten
Azpeitia endoi (Kanaya) P. A. Sims and G. A. Fryxell
Azpeitia tabularis (Grunow) G. Fryxell and P. A. Sims
Chaetoceros spp.
Chaetoceros atlanticus Cleve
Chaetoceros breve Schütt
Chaetoceros bulbosus (Ehrenberg) Heiden
Chaetoceros castracanei Karsten
Chaetoceros constrictus Gran
Chaetoceros convolutus Castracane
Chaetoceros criophilus Castracane
Chaetoceros curvisetus Cleve
Chaetoceros dichaeta Ehrenberg
Chaetoceros sp. cf. *dichaeta* (Hyalochaete)
Chaetoceros flexuosus Mangin
Chaetoceros neglectus Karsten
Chaetoceros neogracile Van Landingham
Chaetoceros pacificus sensu Semina
Chaetoceros pendulus Karsten
Chaetoceros peruvianus Brightwell
Chaetoceros radicans Schütt
Chaetoceros resting spore (spiny)
Chaetoceros resting spore (smooth)
Chaetoceros sp. cf. *wighamii* Van Heurck
Cocconeis fasciolata (Ehrenberg) Brown
Corethron spp.
Corethron criophilum Castracane
Corethron inerme Karsten
Coscinodiscus spp.
Coscinodiscus curvatulus Grunow *in* Schmidt
Coscinodiscus elliptopora Donahue
Coscinodiscus oculoides Karsten
Dactyliosolen antarcticus Castracane
Dactyliosolen tenuijunctus (Manguin) Hasle
Denticula sp.
Eucampia antarctica (Castracane) Mangin
Haslea spp.
Hemidiscus karstenii Jouse
Leptocylindrus mediterraneus (H. Peragallo) Hasle
Melosira spp.
Navicula directa (Wm. Smith) Ralfs
Nitzschia angulata Hasle
Nitzschia closterium (Ehrenberg) Wm. Smith
Nitzschia curta (Van Heurck) Hasle
[a]*Nitzschia cylindrus* (Grunow) Hasle
Nitzschia heimii Manguin
Nitzschia inflatula Hasle
Nitzschia kerguelensis (O'Meara) Hustedt
Nitzschia lecointei Van Heurck
Nitzschia lineola Cleve
Nitzschia obliquecostata (Van Heurck) Heiden
Nitzschia panduriformis Gregory
Nitzschia prolongatoides Hasle
Nitzschia pseudonana Hasle
Nitzschia ritscheri (Hustedt) Hasle
Nitzschia separanda (Hustedt) Hasle
Nitzschia spp. (ribbon colonies)
Nitzschia spp. (pseudonitzschia chains)
Nitzschia subcurvata Hasle
Nitzschia sublineata Hasle
Nitzschia turgidula Hustedt
Nitzschia turgiduloides Hasle
Odontella weissflogii (Janisch) Grunow
Paralia sulcata (Ehrenberg) Cleve
Pleurosigma spp.
Porosira glacialis (Grunow) Jorgensen
Porosira pseudodenticulata (Hustedt) Jousé
Rhizosolenia alata Brightwell
Rhizosolenia alata forma *inermis* (Castracane) Hustedt (blunt)
Rhizosolenia alata forma *indica* (H. Peragallo) Hustedt (long, rostrate)
Rhizosolenia chunii Karsten
Rhizosolenia crassa Schimper ex Karsten

Table 8 (continued).

Diatoms (Cont.)
Rhizosolenia curvata Zacherias
Rhizosolenia cylindrus Cleve
Rhizosolenia hebetata forma *semispina* (Hensen) Gran
Rhizosolenia simplex Karsten
Rouxia isopolica Schrader
Rouxia naviculoides Schrader
Rouxia spp.
Stellarima microtrias Hasle and Sims
Stictodiscus sp.
Synedra reinboldii? Van Heurck
Thalassionema nitzschoides (Grunow) Hustedt
Thalassiosira sp.
Thalassiosira sp. cf. *sensu* Schrader
Thalassiosira ambigua Kozlova
Thalassiosira australis M. Peragallo
Thalassiosira frenguellii Kozlova
Thalassiosira frenguelliopsis Fryxell and Johansen
Thalassiosira gerloffii Rivera
Thalassiosira gracilis forma *expecta* (Van Landingham) G. Fryxell and Hasle
Thalassiosira gracilis forma *gracilis* (Karsten) Hustedt
Thalassiosira gravida Cleve
Thalassiosira lentiginosa (Janisch) Fryxell
Thalassiosira maculata Fryxell and Johansen
Thalassiosira oestrupii (Ostenfeld) Hasle
Thalassiosira oliverana (O'Meara) Makarova and Nikolaev
Thalassiosira perpusilla Kozlova
Thalassiosira ritscheri (Hustedt) Hasle
Thalassiosira scotia Fryxell and Hoban
Thalassiosira trifulta Fryxell ex Fryxell and Hasle
Thalassiosira tumida (Janisch) Hasle
Thalassiosira antarctica (Schimper
Trichotoxin reinboldii (Van Heurck) Reid and Round
Tropidoneis antarctica (Grunow) Cleve
Tropidoneis belgicae (Van Heurck) Heiden and Kolbe
Tropidoneis gausii Heiden
Tropidoneis glacialis Heiden et Kolbe
Silicoflagellates
Distephanus speculum (Ehrenberg) Haeckel
Prymnesiophytes
Phaeocystis pouchetti (Hariot) Langerheim

[a] *Nitzschia cylindrus* was described as *Fragilaria cylindrus*, meaning "*Fragilaria*, the cylinder." "Cylindrus" is thus a noun in apposition, both with *F. cylindrus* and the combination *N. cylindrus*. *Nitzschia "cylindra"* now in same use is artificial Latin, and we see no reason to change *N. cylindrus*. (See International Code of Botanical Nomenclature, Articles 23.5 and 73.1.)

Article 23.5—"The specific epithet, when adjectival in form and not used as a substantive, agrees grammatically with the generic name."

"Ex. 4, *Helleborus niger, Brassica nigra, Verbascumnigrum; Vinca major, Tropreolum majus; Rubus amnicola.* The specific epithet being a Latin substantive; *Peridermium balsameum* Peck, but also *Gloeosporium balsameae* J. J. Davis, both derived from the epithet of *Abies balsamea*, the specific epithet of which is treated as a substantive in the second example."

Article 73.1—"The original spelling of a name or epithet is to be retained, except for the correction of typographic or orthographic errors."

We used high-performance liquid chromatography (HPLC) (Abaychi and Riley, 1979; Mantoura and Llewellyn, 1983; Bidigare et al., 1985) to measure pigment concentrations. From 2 to 4 L of water from each sample was filtered onto Nucleopore polyester filters (pore size 0.4 μm) that were immediately frozen. These filters were examined using HPLC at Texas A&M University for the presence and concentration of chlorophylls *a*, *b*, and *c* and their degradation products (phaeophytins, phaeophorbides, and chlorophyllides).

PHYSICAL PROPERTIES

The shipboard physical-properties program was aimed at monitoring variations in geotechnical properties of the different lithologic units cored. Measured properties included bulk and grain density, compressional wave velocity, thermal conductivity, undrained shear strength, water content, and porosity. Measurements generally were carried out at sufficiently dense intervals to fully cover different lithologic units. The physical-properties data contain important information about the nature of the different lithologies in regards to the degree of consolidation and slope stability. Particularly for the program in Prydz Bay, the consolidation history of the cored sediments is an important parameter. Furthermore, density and velocity measurements were combined to give acoustic parameters that, through construction of synthetic seismograms, are essential in correlating cored units to seismic profiles and downhole logging results. Taylor (1984) and Eldholm, Thiede, et al. (1987) have demonstrated the usefulness of depth profiles of geotechnical properties in distinguishing lithologic boundaries at drill sites as well as in correlating and establishing facies changes between sites (geotechnical stratigraphy).

A detailed discussion of physical properties with respect to equipment, methods, errors, correction factors, and problems related to coring disturbance was presented by Boyce (1976). A brief review of the methods used during Leg 119 is given here. The methods are discussed in the same sequence as the analyses were performed in the shipboard laboratory. Any site-specific deviations from procedures below are discussed in the individual site chapters.

Gamma-Ray Attenuation Porosity Evaluator (GRAPE)

Wet-bulk density is calculated from the attenuation of a gamma ray passing through the diameter of the core. Internal, computational constants are set by running an aluminum standard, and this was done at least once per site during Leg 119.

The GRAPE was run on the entire length of all cores in which the sediment completely filled the liner. As the system is calibrated for standard liner diameter, densities measured on material that does not fill the liner will be erroneous. This often is the case in RCB-cored lithified material and was a general problem at most of the Prydz Bay sites. For such material, GRAPE density was measured on discrete samples of known thickness by 2-min exposure to the gamma-ray beam (2-min GRAPE).

A shipboard software package processing of the continuously run GRAPE data includes merging of individual files (one per section), adding real depths below seafloor, filtering, and blocking. During Leg 119, filter low and high cuts were set to 1.0 and 3.0 g/cm^3, respectively, to remove obviously erroneous data points. The data were then blocked into intervals of 0.1 to 0.5 m before they were graphically displayed.

P-Wave Logger (PWL)

The PWL was designed and built at the Institute of Oceanographic Sciences, Wormley, UK, to obtain continuous velocity readings throughout the cored sequence. The transducers are mounted in the GRAPE system and are aligned perpendicular to the gamma ray. Compressional-wave velocity (V_p) is measured in pre-set intervals along the whole-round core. A 500-kHz pulse is produced at a repetition rate of 1 kHz at the transmitter and is detected by the receiver with an accuracy of 50 ns. The system consists of a Tektronix DC 5010 counter/timer, Tektronix SC 504 oscilloscope, power supply, and amplifier. After suitable calibration, V_p is computed and logged on a DEC PRO-350 computer. This should allow relative velocity changes to be detected with a resolution of 1.5 m/s, while the absolute accuracy is about 5 m/s due primarily to variable thickness of the core liner.

The sampling interval was set to 2 cm, which had proved to be an adequate interval during previous tests. Suitable coupling between the transducers and the liner was achieved by spraying the liner with salt and water. However, as the coupling between the liner and the core proper is equally important, the PWL is

generally used only for HPC cores. Similar to the GRAPE, the PWL system requires good coupling between the liner and the cored material. Hence, both the PWL and continuous GRAPE runs were mostly carried out on HPC-cored sediments, and particularly at the Prydz Bay sites, PWL data are sparse.

Processing of the PWL data involved the same software and included the same steps as for the GRAPE. Filtering of the PWL data was done on a dimensionless number representing signal strength. Values below a certain limit were removed, thereby removing measurements with poor coupling between the sample and the liner.

Thermal Conductivity

Thermal-conductivity data are collected by inserting up to four needle probes (Von Herzen and Maxwell, 1959) through small holes drilled in the core liner. These probes are connected to a Thermcon-85 unit mated to a PRO-350 computer system. This system computes the coefficient of conductivity as a function changes in resistance in the needles induced by changes in temperature over a 6-min interval. One probe is inserted in a rubber standard and run with each set of measurements. A drift of less than 4×10^{-2}°C/min is essential for reliable data. This requires allowing core sections to thermally equilbrate for approximately 4 hr prior to analysis.

Thermal-conductivity data were collected at eight of the 11 Leg 119 sites. The system has connectors for up to five needle probes, and the common procedure was to measure at four levels per core while the fifth needle was placed in the rubber standard. However, we were careful to cover different lithologies, as seen from density contrasts on the GRAPE records.

Shear-Strength Measurements

Vane Shear Strength

The shipboard instrument used is a modified Wykeham Farrance Laboratory Vane Apparatus, which is a small (1.27 × 1.27 cm) four-bladed vane that is inserted into the sample and rotated at a speed of 89°/min until a peak torque is reached. The torque sensor is a calibrated spring. An undrained shear strength (Su) is calculated assuming full-strength mobilization along a circular cylinder inscribed about the vane. The method is thoroughly discussed by Lee (1984).

Tests are performed in regions of minimum sample disturbance and are at least dense enough to cover all variations in lithofacies. The blade is inserted perpendicular to split-core faces and, hence, parallel to bedding planes, which is a practical compromise, although not ideal. Furthermore, to avoid the presumably more disturbed outer zone along the liner, the vane was inserted to a depth where the top of the blade was just covered by sediment, whereas the optimal is insertion to a depth at least equal to the blade height (Lee, 1984). However, we were careful to make consistent measurements throughout the cruise.

The motorized vane is generally limited to material of shear strengths below 70 kPa and does not give reliable results in unsorted, gravelly diamictons. In these sediments, fall cone and pocket penetrometers were used. In firm sediments the motor of the apparatus started to fail, and peak torque occasionally had to be reached by rotating the vane manually.

Fall Cone Penetrometer

This device, produced by Soiltest Inc., is used by placing a cone of given apex angle and weight with the cone apex touching the sediment surface. The cone is released from its holder, and its penetration into the sediment is measured in millimeters. The undrained shear strength can be determined (Hansbo, 1957) using empirical conversion tables.

Four cones were used—10 g/60°, 60 g/60°, 100 g/30°, and 400 g/30°—covering shear strengths in the range of 0.1 to 370 kPa. At least two tests were performed at each measured level and the readings averaged to give the shear strength. In poorly sorted sediments, particularly the Prydz Bay diamictons, more than two tests were necessary.

Pocket Penetrometer

With this instrument, also manufactured by Soiltest Inc., a small flat-footed cylindrical probe is pushed 6.4 mm into the sediment and a seal provides a direct read-out of unconfined compressional strength (2 × Su), based on empirical relations. The instrument is particularly convenient for rapid testing of very firm material. The penetrometer used during Leg 119 is provided by the Norwegian Geotechnical Institute and equipped with adapters that increased the maximum measurable shear strength from 225 to 900 kPa. Two to five readings were done at each measured level, to ensure representative shear strength values.

Hamilton Frame Compressional-Wave Velocity

Compressional-wave velocity was, in addition to the PWL system (described previously), also measured in a Hamilton Frame Velocimeter. The unit consists of two frame-mounted transducers using a transmitter frequency of 500 kHz. Traveltime through the sample is measured on a Tektronix DC 5010 counter/timer system and a Tektronix 5110 oscilloscope. Travel distance was measured by a Dial Micrometer attached to the upper transducer.

In unlithfied sediments, measurements were performed through split-core sections, correcting for liner thickness and velocity adjacent to shear strength and index properties sites. Hence, the measurements were done parallel to the bedding planes. In firm and lithified material, the measurements were done on the discrete samples used for the 2-min GRAPE measurements. A number of these samples were measured both parallel and perpendicular to the bedding planes for velocity anisotropy analyses.

Index Properties

Salt-corrected index properties (water content, wet- and dry-bulk densities, porosity, and grain density), were computed for samples of 3–7 cm^3 volume, assuming a pore-water salinity of 35 ppt. Water contents are expressed as the percentage ratio of water to wet sample. Sample weights were measured on an electronic balance system, calibrated against standard averaging 100–300 counts, or on a triple-beam balance. Volumes were measured from a Penta-Pycnometer (Quantachrome Corp.) using helium as the purging gas. Dry weights and volumes were determined after 12 hr of freeze drying. A section of the freeze-dried samples was later used for carbonate content analyses (see "Inorganic Geochemistry," this chapter). All samples were measured in numbered aluminum beakers designed for the Penta-Pycnometer. Weights and volumes of all beakers used during Leg 119 were measured prior to drilling.

Sampling for index properties was usually done adjacent to all other physical-properties-analyses sites. Occasionally, index properties were measured at denser intervals than the other analyses. Particularly in the poorly sorted Prydz Bay diamictons and diamictites, we tried to take numerous, as large as possible samples to assure that we obtained representative results.

LOGGING

The purpose of downhole logging is the direct determination of properties of *in-situ* formations adjacent to the borehole wall. Geophysical log data are recorded using probes lowered on the end of a wireline through the drill pipe and into the previ-

ously drilled borehole. Two standard Schlumberger tool combinations were used on Leg 119: the seismic stratigraphic combination and the lithoporosity combination.

Log Types

Seismic Stratigraphic Combination

The seismic stratigraphic combination includes the long-spacing sonic (LSS), dual induction (DIL), gamma-ray (GR), and caliper (MCD) tools. Its value to seismic stratigraphy is that it directly measures compressional-wave sound velocity and indirectly measures the two variables that most commonly affect velocity: porosity and clay mineral percentage.

Dual Induction Resistivity Log (DIL)

The DIL is a resistivity logging device that provides measurements of spontaneous potential (SP) and three resistivity values, each with a different depth of investigation: ILD (deep induction), ILM (medium induction), and SFLU (shallow spherically focused resistivity). Because the solid constituents are orders of magnitude more resistive than the pore fluids in most rocks, resistivity is controlled mainly by the amount and connectivity of the porosity and the conductivity of the pore fluids.

Sonic porosity is a measure of the streaming potential generated by the differences between borehole and pore-fluid electrical properties, from which both membrane and liquid junction potentials result from the differences in ion mobility in the formation and drilling fluids. The induction sonde consists of a series of transmitter coils excited by a high-frequency (25-kHz) sinusoidal current and a series of detector coils. In a nonconducting medium the electromagnetic field induced in the detector coils by the transmitting coils is balanced between coil pairs. In a conducting medium the magnetic field produced by currents induced in the surrounding material induces additional currents in the receivers, changing the amplitude and phase of the total induced current. The depth of investigation is between 0.5 and 5 m, and the vertical resolution about 1.5 m.

The resistivity measured by the induction log is quite accurate for low (less than 100 ohm-m) resistivities, but for more resistive formations it reads too low by as much as 50%. In these rocks the focused resistivity log produces more reliable results. The SFLU consists of a transmitter coil and a series of focusing coils that force current into the formation laterally away from the borehole. Without these field-shaping coils, current would tend to be conducted exclusively within the borehole. The SFLU provides a direct measurement of formation resistivity about 1 m from the well bore, with a vertical resolution of about 0.6 m.

Long-Spaced Sonic (LSS)

The sonic tool is designed to measure the elastic compressional-wave velocity of the formation surrounding the borehole. In essence, the sonic tool can be thought of as a miniature seismic-refraction experiment carried out within the cylindrical borehole. The tool, containing one or more sources and receivers, is centered in the hole by bow springs. A source fires acoustic energy that is transmitted into the borehole fluid. When the wavefront impinges on the borehole wall, a refracted compressional wave is generated. If the formation shear velocity is higher than the acoustic velocity of the fluid, a refracted shear wave will also be generated. The refracted waves travel along the borehole wall, reradiating energy into the fluid. Energy arrives at receivers on the logging tool at a time linearly proportional to their offset from the source. Formation elastic-wave velocities thus can be determined from the difference between the arrival times at two receivers a known distance apart.

The Schlumberger LSS sonde uses two acoustic transmitters spaced 2 ft apart and two receivers also spaced 2 ft apart and located 8 ft above the transmitters. This arrangement provides four source-receiver offsets of 8, 10, and 12 ft. Compensation for borehole irregularities and the inclination of the tool to the hole axis is achieved by averaging the first transit-time reading with a second reading obtained after the sonde has been raised a fixed distance along the borehole. The LSS tool records the full waveform for each source-receiver pair, in addition to automatically determining its arrival time.

Compressional sonic velocity is one of the primary elastic properties measured during logging. The product of velocity and density (impedance) is useful in computing synthetic seismograms for time-depth ties of seismic reflectors.

Natural Gamma Ray (GR)

The Schlumberger GR probe uses a scintillation detector to measure the natural radiation emitted by the rocks surrounding the borehole. This radiation arises from naturally occurring radioisotopes of the potassium, thorium, and uranium decay series. The detector is a sodium iodide crystal. Gamma response is influenced by hole size and by the density of the drilling fluid. Thus, its response must be corrected using caliper data. The average investigation depth into sedimentary formations is about 1 ft. The GR is used principally as a depth correlator between logging runs. Because radioactive elements are concentrated in clays, micas, and feldspar, the standard gamma-ray log also provides an indication of the relative abundance of these minerals.

Caliper Log (MCD)

The Schlumberger MCD is run at the top of the seismic stratigraphic combination and measures the size of the well bore. Extension of the three bow springs mounted 120° apart on the tool moves a contact along a potentiometer. Changes in the resistance of the potentiometer are linearly proportional to the hole size. The caliper has an extension of 16 in., so large-diameter "washouts" are not measured accurately.

The caliper is primarily used to indicate bad parts of the hole, where other logs may read inaccurately, and to correct the responses of those logs sensitive to less severe variations in hole size. The caliper response can also be indicative of lithology. For instance, in zones with swelling clays, hole constrictions are observed where the caliper reads less than the bit size. In addition, as hole conditions in general are a consequence of rock properties, variations in hole size may correlate with lithologic changes.

Lithoporosity Combination

The lithoporosity combination includes the natural gamma spectrometry (NGT), lithodensity (LDT), and compensated neutron (CNT-G) tools. This combination measures formation porosity and density as well as estimates of the proportions of the primary radioactive elements (U, K, and Th).

Dual-Porosity Neutron Log (CNT-G)

The CNT-G contains two detectors and a chemical source (Am-Be) with an average energy of 5 Mev neutrons. The neutrons produced by this source collide with atoms in the formation and are scattered. Collisions with heavy atoms do not exchange much energy, but collisions with hydrogen can cause the neutrons to move very slowly. When the neutrons reach a low energy level (0.025 Mev) they can be captured by the nuclei of elements such as chlorine, lithium, boron, or gadolinium, and gamma rays of capture are emitted. By comparing the flux of neutrons returning to two detectors at different distances from the source, the neutron log provides primarily a measure of the hydrogen content of the formation. The measure of hydrogen content is transformed into porosity, based on the assumption

that water fills the porous medium. The vertical resolution of the tool is about 0.25 m.

Natural Gamma-Ray Spectrometry Log (NGT)

The NGT utilizes a sodium-iodide detector to determine the spectral content of naturally occurring radiation. The entire spectrum is transmitted to the surface, and the energy arriving in five preselected windows is measured by the surface electronics. The concentrations of potassium, uranium, and thorium are determined by analysis of the energy in the five bands. The spectral gamma log is commonly referred to as a KUT (K, U, and Th) log. The concentration of thorium in ppm is determined directly, whereas the concentrations of uranium in ppm and potassium in weight percent are determined by a stripping technique.

The relative proportions of K, Th, and U are controlled by the mineralogy, clay content, and alteration history. Clay type is determined from the relative abundances of thorium and potassium, the primary radioactive elements in clay. Uranium is commonly associated with organic matter in carbonate. The vertical resolution of the tool is about 0.25 m.

Lithodensity Log (LDT)

The Schlumberger LDT contains a chemical source (^{137}Ce) of 0.66 Mev gamma rays. As modified for ODP use, a pair of detectors and the source mounted in the tool body are forced against the borehole wall by a bow spring. The two detectors measure the flux of transmitted gamma rays in a series of energy windows to determine density (RHOB) and photoelectric factor (PEF). A measure of tool performance based on the energy distribution at the near and far receivers (DRHO) is also provided. Gamma rays with energies less than 1.01 Mev interact with atoms in the formation by Compton scattering and via the photoelectric effect. Compton scattering is an elastic collision by which energy is transferred between the gamma ray and electron in the formation. This interaction forms the basis of the density measurement. In effect, the LDT measures electron density directly, and formation density is determined using the fact that the atomic weight is approximately twice the atomic number in most rock-forming elements. At low energies (below about 0.06 Mev) gamma rays are subject to absorption via the photoelectric effect. One of the energy windows on the far detector is tuned to measure this effect, and the measurement is inverted to obtain the PEF determination. Because this measurement is almost independent of porosity it can be used directly as a matrix lithology indicator.

The depth of investigation of the lithodensity tool depends on the density of the rock: the higher the density, the lower the penetration. In porous and permeable formations the density tool does not read deeper than 0.16 m. The vertical resolution is about 0.3 m.

During Leg 119 two additional measurements were included with the lithoporosity combination for temperature (AMS) and magnetism and inclinometry (GPIT).

GPIT Cartridge

This tool determines the hole azimuth and deviation and the vector components of the magnetic field. Although it is not oriented gyroscopically, the GPIT can accurately measure the magnetic field inclination. The device also monitors vertical and horizontal accelerations applied to the logging probe and thus can be used to determine the effects of ship heave on the logging run.

Data Acquisition and Computer Analysis

The computer on the Schlumberger recording sled is designed primarily for data acquisition and display of the primary log curves. However, it can run a few analyses to obtain a "quick look" at computed values. In general the Schlumberger computer is used only for data acquisition and to produce clean data tapes and log playbacks for the shipboard party.

The Masscomp logging computer in the downhole measurements laboratory runs a log analysis package called Terralog, which is an interactive system consisting of a large number of log manipulation and plot options. Preliminary log interpretation as well as display in standard log format can be carried out aboard ship; more detailed analysis is done by the Borehole Research Group at Lamont-Doherty Geological Observatory.

Synthetic Seismogram

Synthetic seismograms were computed at sites where downhole sonic and density logs were recorded to provide correlation of vertical incidence seismic-reflection data with subsurface cores. The synthetic seismogram is derived through convolution of a seismic source wavelet with subsurface acoustic impedance (product of density and velocity). The resulting waveform can be compared with the vertical-incident seismic-reflection profile to determine approximate depths to reflectors (e.g., geologic horizons).

In practice, synthetic seismograms are commonly computed solely from downhole sonic logs and other velocity information because (1) velocity has a greater effect than density on acoustic impedance because of larger percentage variations in velocity and (2) velocity and density are normally strongly correlated, giving similar variations. On Leg 119, the seismograms were computed using all reliable density and velocity information.

The seismic wavelet used for computing the synthetic seismograms is the direct-arrival signature of the *Resolution*'s two water gun array, as measured by the seismic streamer (e.g., source-to-receiver; Fig. 11). This wavelet closely resembles that recorded from the seafloor in areas of flat-lying strata, thereby providing a good far-field signature of the source array. The 70-m wavelet was recorded using a filter band-pass of 25 to 250 Hz and was sampled at 2-ms intervals for use in the seismogram computation.

The synthetic seismogram was computed using a simple one-dimensional convolution algorithm (R. Jarrard, pers. comm, 1988). The algorithm computes internal multiples, but not pri-

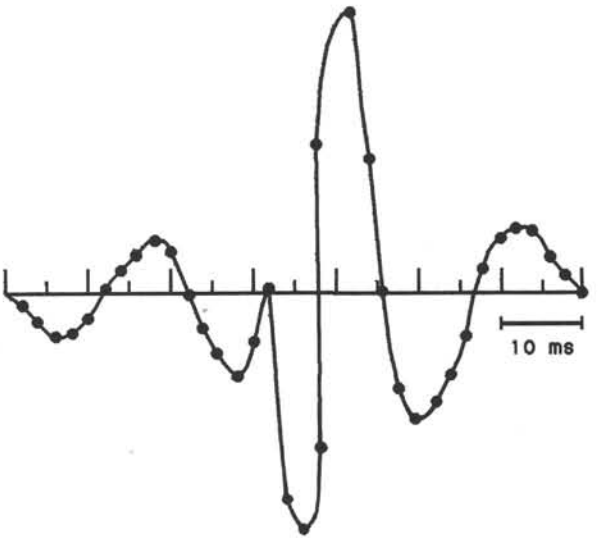

Figure 11. Seismic wavelet used in computing the synthetic seismogram.

mary seafloor multiples. The seafloor multiple was not a problem on Leg 119, however, because drilling did not reach subsurface times (depths) equivalent to that for the first seafloor multiple. Synthetic seismograms are not filtered and thus show relatively high-frequency (25–250-Hz) synthetic seismic traces.

The seismic sections used for comparison with the synthetic seismogram have been filtered from 25 to 180 Hz to eliminate coherent electrical noise of 220 Hz in the raw seismic data. The observed seismic trace selected for comparison is 244 shotpoints from the shotpoint at which the site beacon was dropped. The reader is referred to Figure 25 in the "Underway Geophysics" chapter (this volume) for an illustration of the reflection geometry at beacon drop.

REFERENCES

Abaychi, J. K., and Riley, J. P., 1979. The determination of phytoplankton pigments by high-performance liquid chromatography. *Anal. Chim. Acta*, 107:1–11.

Baldauf, J. G., 1984. Paleoceanography of the Rockall Plateau Region, North Atlantic, Deep Sea Drilling Project Leg 81. *In* Roberts, D. G., Schnitker, D., et al., *Init. Repts. DSDP*, 81: Washington (U.S. Govt. Printing Office), 439–465.

Barker, P. F., Kennett, J. P., et al., 1988. *Proc. ODP, Init. Repts.*, 113: College Station, TX (Ocean Drilling Program).

Barrett, P. J., Hambrey, M. J., and Robinson, P. H., in press. Cenozoic glacial and tectonic history from CIROS-1, McMurdo Sound. *In* Thompson, M.R.A. (Ed.), *5th International Antarctic Earth Science Symposium Volume*: Cambridge (Cambridge Univ. Press).

Barron, J. A., 1985. Late Eocene to Holocene diatom biostratigraphy of the equatorial Pacific Ocean, Deep Sea Drilling Project Leg 85. *In* Mayer, L., Theyer, F., et al., *Init. Repts. DSDP*, 85: Washington (U.S. Govt. Printing Office), 413–456.

Bates, R. L., and Jackson, J. A., 1980. *Glossary of Geology* (2nd ed.): Falls Church, VA (American Geological Inst.).

Berggren, W. A., 1969. Rates of evolution of some Cenozoic planktonic foraminifera. *Micropaleontology*, 15:351–365.

Berggren, W. A., Kent, D. V., and Flynn, J. J., 1985a. Paleogene geochronology and chronostratigraphy. *In* Snelling, N. J. (Ed.), *Geochronology of the Geological Record*: Geol. Soc. London Mem., 10: 141–195.

Berggren, W. A., Kent, D. V., Flynn, J. J., and Van Couvering, J. A., 1985b. Cenozoic geochronology. *Geol. Soc. Am. Bull.*, 96:1407–1418.

Berggren, W. A., Kent, D. V., and Van Couvering, J. A., 1985c. The Neogene: Part 2. Neogene geochronology and chronostratigraphy. *In* Snelling, N. J. (Ed.), *Geochronology of the Geological Record*: Geol. Soc. London Mem., 10:211–260.

Bernard, B. B., Brooks, J. M., and Sackett, W. N., 1978. Light hydrocarbons in recent Texas continental shelf and slope sediments. *J. Geopys. Res.*, 83:4053–4061.

Bidigare, R. R., Kennicutt, M. C., and Brooks, J. M., 1985. Rapid determination of chlorophylls and degradation products by high-performance liquid chromatography. *Limnol. Oceanogr.*, 30:432–435.

Blow, W. H., 1969. Late middle Eocene to Recent planktonic foraminiferal biostratigraphy. *In* Bronniman, R., and Renz, H. H. (Eds.), *Proc. 1st Int. Conf. Planktonic Microfossils*: Leiden (E. J. Brill), 199–421.

_____, 1979. *The Cenozoic Foraminifera*: Leiden (E. J. Brill).

Bolli, H., and Saunders, J., 1985. Oligocene to Holocene low latitude planktic formaninfera. *In* Bolli, H. M., Saunders, J. B., and Perch-Nielsen, K. (Eds.), *Plankton Stratigraphy*: Cambridge (Cambridge Univ. Press), 155–262.

Boltovskoy, E., 1978. Late Cenozoic benthonic Foraminifera of the Nineteast Ridge (Indian Ocean). *Mar. Geol.*, 26:139–178.

Boyce, R. E., 1976. Definitions and laboratory techniques of compressional sound velocity parameter and water content, wet-bulk density, and porosity parameters by gravimetric and gamma ray attenuation techniques. *In* Schlanger, S. O., Jackson, E. D., et al., *Init. Repts. DSDP*, 33: Washington (U.S. Govt. Printing Office), 931–955.

Bukry, D., 1973. Low-latitude coccolith biostratigraphic zonation. *In* Edgar, N. T., Saunders, J. B., et al., *Init. Repts. DSDP*, 15: Washington (U.S. Govt. Printing Office), 685–703.

_____, 1975. Coccolith and silicoflagellate stratigraphy, northwestern Pacific Ocean, Deep Sea Drilling Project Leg 32. *In* Larson, R. L., Moberly, R., et al., *Init. Repts. DSDP*, 32: Washington (U.S. Govt. Printing Office), 677–701.

Burckle, L. H., 1978. Early Miocene to Pliocene diatom datum levels for the equatorial Pacific. *In Biostratigraphic Datum-Planes of the Pacific Neogene*: IGCP Proj. 114 Proc. Spec. Publ. Repub. Indo. Minist. Mines Energy, 1:25–44.

Burckle, L. H., Clarke, D. B., and Shackleton, N. J., 1978. Isochronous last abundance appearance datum (LAAD) of the diatom *Hemidiscus karstenii* in the Sub-Antarctic. *Geology*, 6:243–236.

Caron, M., 1985. Cretaceous planktonic foraminfera. *In* Bolli, H. M., Saunders, J. B., and Perch-Neilsen, K. (Eds.), *Plankton Stratigraphy*: Cambridge (Cambridge Univ. Press), 17–86.

Caulet, J. P., 1985. Radiolarians from the southwest Pacific. *In* Kennett, J. P., von der Borch, C. C., et al., *Init. Repts. DSDP*, 90: Washington (U.S. Govt. Printing Office), 835–861.

_____, 1986. A refined radiolarian biostratigraphy for the Pleistocene of the temperate Indian Ocean. *Mar. Micropaleontol.*, 11:217–229.

Chen, P. H., 1975. Antarctic radiolaria. *In* Hayes, D. E., Frakes, L. A., et al., *Init. Repts. DSDP*, 28: Washington (U.S. Govt. Printing Office), 407–474.

Ciesielski, P. F., 1983. The Neogene and Quaternary diatom biostratigraphy of subantarctic sediments, Deep Sea Drilling Project Leg 71. *In* Ludwig, W. J., Krasheninnikov, V. A., et al., *Init. Repts. DSDP*, 71: Washington (U.S. Govt. Printing Office), 635–665.

Douglas, R. G., 1973. Benthonic foraminiferal biostratigraphy in the central North Pacific, Leg 17, DSDP. *In* Winterer, E. L., Ewing, J. I., et al., *Init. Repts. DSDP*, 17: Washington (U.S. Govt. Printing Office), 607–671.

Dreimanis, A., 1979. The problem of waterlain tills. *In* Schliichter, C. (Ed.), *Moraines and Varves*: Rotterdam (A. A. Balkema), 166–177.

Eldholm, O., Thiede, J., et al., 1987. *Proc. ODP, Init. Repts.*, 104: College Station, TX (Ocean Drilling Program).

Emeis, K. C., and Kvenvolden, K. A., 1986. Shipboard organic geochemistry on *JOIDES Resolution*. *ODP Tech. Note*, 7.

Evans, C. A., O'Reilley, J. E., and Thomas, J. P., 1987. A handbook for the measurement of chlorophyll and primary production. *Biomass*, 8.

Fenner, J., 1985. Late Cretaceous to Oligocene planktonic diatoms. *In* Bolli, H. M., Saunders, J. B., and Perch-Neilsen, K. (Eds.), *Plankton Stratigraphy*: Cambridge (Cambridge Univ. Press), 713–762.

Flint, R. F., Saunders, J. E., and Rudsans, J., 1960. Diamictite, a substitute term for symmictite. *Geol. Soc. Am. Bull.*, 71:1809.

Foreman, H. P., 1977. Mesozoic Radiolaria from the Atlantic basin and its borderlands. *In* Swain, F. M. (Ed.), *Stratigraphic Micropaleontology of Atlantic and Borderlands*: Amsterdam (Elsevier), 305–320.

Fryxell, G. A., 1975. Morphology, taxonomy, and distribution of selected species of the diatom genus *Thalassiosira Cleve* in the Gulf of Mexico and Antarctic waters [Ph.D. dissert.]. Texas A&M Univ.

Gieskes, J. M., 1974. Interstitial water studies, Leg 25. *In* Simpson, E.S.W., Schlich, R., et al., *Init. Repts. DSDP*, 25: Washington (U.S. Govt. Printing Office), 361–394.

Gieskes, J. W., and Peretsman, G., 1986. Water chemistry procedures aboard the *JOIDES Resolution*–some comments. *ODP Tech. Note, 5*.

Gombos, A. M., and Ciesielski, P. F., 1983. Late Eocene to early Miocene diatoms from the southwest Atlantic. *In* Ludwig, W. J., Krasheninnikov, V. A., et al., *Init. Repts. DSDP*, 71: Washington (U.S. Govt. Printing Office) 583–634.

Hambrey, M. J., Barrett, P. J., Hall, R. J., and Robinson, P. H., in press. Stratigraphy. *In* Barrett, P. J. (Ed.), *Cenozoic History of McMurdo Sound, Antarctica from CIROS-1 Drill-Hole*: DSIR Bull. (N. Z.).

Hambrey, M. J., and Harland, W. B., 1981. *Earth's Pre-Pleistocene Glacial Record*: Cambridge (Cambridge Univ. Press).

Hansbo, S., 1957. A new approach to the determination of the shear strength of clay by the fall-cone test. *Swed. Geotech. Inst., Publ.*, 14.

Helby, R., Morgan, R., and Partridge, A. D., 1987. A palynological zonation of the Australian Mesozoic. *In* Jell, P. A. (Ed.), *Studies in Australian Mesozoic Palynology*: Assoc. Aust. Palynol., Mem. 4:1–45.

Holm-Hansen, O., Lorenzen, C. J., Holmes, R. W., and Strickland, J.D.H., 1965. Fluorometeric determination of chlorophyll. *J. Cons., Cons. Int. Explor. Mer*, 30:3–15.

Huber, B. T., in press. Upper Campanian-Paleocene foraminifera from the James Ross Island region (Antarctic Peninsula). *In* Feldmann, R. M., and Woodburne, M. O. (Eds.), *Geology and Paleontology of Seymour Island (Antarctic Peninsula)*: Mem. Geol. Soc. Am., 169.

Jacobsen, T. R., 1982. Comparison of chlorophyll measurements by fluorometric, spectrophotometric, and high pressure liquid chromatographic methods in aquatic environments. *Ergeb. Limnol.*, 16:35–45.

Jenkins, D. G., 1985. Southern and mid-latitude Paleocene to Holocene planktonic foraminifera. *In* Bolli, H. M., Saunders, J. B., and Perch-Neilsen, K. (Eds.), *Plankton Stratigraphy*: Cambridge (Cambridge Univ. Press), 263–282.

Jenkins, D. G., and Srinivasan, M. S., 1986. Cenozoic planktonic foraminifers of the southwest Pacific. *In* Kennett, J. P., von der Borch, C. C., et al., *Init. Repts. DSDP*, 90: Washington (U.S. Govt. Printing Office), 795–834.

Kvenvolden, K. A., and McDonald, T. J., 1986. Organic geochemistry aboard the *JOIDES Resolution*–an assay: *ODP Tech. Note*, 6.

Kvenvolden, K. A., and Redden, G. D., 1980. Hydrocarbon gas in sediment from the shelf, slope, and basin of the Bering Sea. *Geochim. Cosmochim. Acta*, 44:1145–1150.

Leckie, R. M., and Webb, P. N., 1986. Late Paleogene and early Neogene foraminifers of Deep Sea Drilling Project Site 270, Ross Sea, Antarctica. *In* Kennett, J. P., von der Borch, C. C., et al., *Init. Repts. DSDP*, 90: Washington (U.S. Govt. Printing Office), 1093–1142.

Lee, H. J., 1984. State of the art: laboratory determination of strength of marine soils. *In* Chaney, R. C., and Demars, K. R. (Eds.), *Strength Testing of Marine Sediments: Laboratory and In-situ Measurements*. ASTM Spec. Tech. Publ. 883:181–250.

Loftus, M. E., and Carpenter, J. H., 1971. A fluorometric method for determining chlorophyll *a, b*, and *c*. *J. Mar. Res.*, 29:319–338.

Manheim, F. T., and Sayles, F. L., 1974. Composition and origin of interstitial waters of marine sediments. *In* Goldberg, E. D. (Ed.), *The Sea*, (vol. 5): New York (Wiley), 527–568.

Mann, R., and Gieskes, J. M., 1975. Interstitial water studies, Leg 28. *In* Hayes, D. E. and Frakes, L. A., et al., *Init. Repts. DSDP*, 28: Washington (U.S. Govt. Printing Office), 805–814.

Mantoura, R.F.C., and Llewellyn, C. A., 1983. The rapid determination of algal chlorophyll and carotenoid pigments and their breakdown products in natural waters by reverse-phase high-performance liquid chromatography. *Analytica Chim. Acta*, 151:297–314.

Martini, E., 1971. Standard Tertiary and Quaternary calcareous nannoplankton zonation. *In* Farinacci, A. (Ed.), *Proc. Planktonic Conf. II Rome 1970*: Rome (Ed. Technoscienze), 739–785.

Matthews, D. J., 1939. *Tables of Velocity of Sound in Pore Water and in Seawater*: London (Admiralty, Hydrogr. Dept.).

Mazzullo, J., Meyer, A. W., and Kidd, R. B., 1987. New sediment classification scheme for the Ocean Drilling Program. *In* Mazzullo, J., and Graham, A. (Eds.), *Handbook for Shipboard Sedimentologists*: ODP Tech. Note 8:44–63.

McCollum, D. W., 1975. Diatom stratigraphy of the Southern Ocean. *In* Hayes, D. E., Frakes, L. A., et al., *Init. Repts. DSDP*, 28: Washington (U.S. Govt. Printing Office), 515–571.

Miller, K. G., and Katz, M. E., 1987. Oligocene to Miocene benthic foraminiferal and abyssal circulation changes in the North Atlantic. *Micropaleontology*, 33:97–149.

Monechi, S., and Thierstein, H. R., 1985. Late Cretaceous–Eocene nannofossil and magnetostratigraphic correlations near Gubbio, Italy. *Mar. Micropaleontol.*, 9:419–440.

Morley, T. J., and Shackleton, N. J., 1978. Extension of the radiolarian *Stylatractus universus* as a biostratigraphic datum to the Atlantic Ocean. *Geology*, 6:309–311.

Nigrini, C., 1971. Radiolaria zones in the Quaternary of the equatorial Pacific Ocean. *In* Funnell, B. M., and Riedel, W. R. (Eds.), *The Micropaleontology of Oceans*: Cambridge (Cambridge Univ. Press), 443–461.

Okada, H., and Bukry, D., 1980. Supplementary modification and introduction of code numbers to low-latitude coccolith biostratigraphic zonation (Bukry, 1973; 1975). *Mar. Micropalentol.*, 5:321–325.

Petrushevskaya, M. G., 1975. Cenozoic radiolarians of the Antarctic, Leg 29, DSDP. *In* Kennett, J. P., Houtz, R. E., et al., *Init. Repts. DSDP*, 29: Washington (U.S. Govt. Printing Office), 541–675.

Riedel, W. R., and Sanfilippo, A., 1974. Radiolaria from the southern Indian Ocean, DSDP Leg 26. *In* Davies, T. A., Luyendyk, B. P., et al., *Init. Repts. DSDP*, 26: Washington (U.S. Govt. Printing Office), 771–814.

Roth, P. H., 1973. Calcareous nannofossils—Leg 17, Deep Sea Drilling Project. *In* Winterer, E. L., Ewing, J. I., et al., *Init. Repts. DSDP*, 17: Washington (U.S. Govt. Printing Office), 695–795.

_____, 1978. Cretaceous nannoplankton biostratigraphy and oceanography of the northwestern Atlantic Ocean. *In* Benson, W. E., Sheridan, R. E., et al., *Init. Repts. DSDP*, 44: Washington (U.S. Govt. Printing Office), 731–759.

Roth, P. H., and Thierstein, H. R., 1972. Calcareous nannoplankton: Leg 14 of the Deep Sea Drilling Project. *In* Hayes, D. E., Pimm, A. C., et al., *Init. Repts. DSDP*, 14: Washington (U.S. Govt. Printing Office), 421–484.

Sanfilippo, A., and Riedel, W. R., 1985. Cretaceous radiolaria. *In* Bolli, H. M., Saunders, J. B., and Perch-Neilsen, K. (Eds.), *Plankton Stratigraphy*: Cambridge (Cambridge Univ. Press), 631–712.

Sanfilippo, A., Westberg, M. J., and Riedel, W. R., 1981. Cenozoic radiolarians at Site 462, Deep Sea Drilling Project Leg 61, western tropical Pacific. *In* Larson, R. L., Schlanger, S. O., et al., *Init. Repts. DSDP*, 61: Washington (U.S. Printing Office), 495–505.

Sanfilippo, A., Westberg-Smith, M. J., and Riedel, W. R., 1985. Cenozoic radiolaria. *In* Bolli, H. M., Saunders, J. B., and Perch-Neilsen, K. (Eds.), *Plankton Stratigraphy*: Cambridge (Cambridge Univ. Press), 631–712.

Schrader, H. J., and Gersonde, R., 1975. Diatoms and silicoflagellates. *Utrecht Micropalentol. Bull.*, 17:129–176.

Shepard, F., 1954. Nomenclature based on sand-silt-clay ratios. *J. Sediment. Petrol.*, 24:151–158.

Tauxe, L., Tucker, P., Petersen, N. P., and LaBrecque, J. L., 1984. Magnetostratigraphy of Leg 73 sediments. *In* Hsü, K. J., LaBrecque, J. L., et al., *Init. Repts. DSDP*, 73: Washington (U.S. Govt. Printing Office), 609–621.

Taylor, E., 1984. Oceanic sedimentation and geotechnical stratigraphy: hemipelagic carbonates and red clays [Ph.D. dissert.]. Texas A&M Univ.

Thomas, E., 1985. Late Eocene to Recent deep-sea benthic foraminifers from the central equatorial Pacific Ocean. *In* Mayer, L., Theyer, F., et al., *Init. Repts. DSDP*, 85: Washington (U.S. Govt. Printing Office), 655–694.

Tissot, B. P., and Welte, D. H., 1984. *Petroleum Formation and Occurrence* (2nd ed.): Berlin (Springer-Verlag).

Tjalsma, R. C., and Lohmann, G. P., 1983. Paleocene-Eocene bathyal and abyssal benthic foraminifera from the Atlantic Ocean. *Micropaleontol. Spec. Publ.*, 4:1–90.

Tourmarkine, M., and Luterbacher, H., 1985. Paleocene and Eocene planktonic foraminifers. *In* Bolli, H. M., Saunders, J. B., and Perch-Neilsen, K. (Eds.), *Plankton Stratigraphy*: Cambridge (Cambridge Univ. Press.), 87–154.

Von Herzen, R. P., and Maxwell, A. E., 1959. The measurement of thermal conductivity of deep-sea sediments by a needle-probe method. *J. Geophys. Res.*, 64:1557–1563.

Weaver, F. M., 1983. Cenozoic radiolarians from the southwest Atlantic, Falkland Plateau region, Deep Sea Drilling Project Leg 71. *In* Ludwig, W. J., Krasheninnikov, V. A., et al., *Init. Repts. DSDP*, 71: Washington (U.S. Govt. Printing Office), 667–679.

Weaver, F. M., and Gombos, A. M., Jr., 1981. Southern high-latitude diatom biostratigraphy. *In* Warme, J. E., Douglas, R. G., and Winterer, E. L. (Eds.), *The Deep Sea Drilling Project: A Decade of Progress*: Spec. Publ. Soc. Econ. Paleontol. Mineral., 32:445–470.

Webb, P. N., 1971. New Zealand Late Cretaceous (Haumurian) foraminifera and stratigraphy: a summary. *N.Z. Geol. Geophys.*, 14:795–828.

_____, 1973. Upper Cretaceous–Paleocene foraminifera from Site 208, DSDP, Leg 21. *In* Burns, R. E., Andrews, J. E., et al., *Init. Repts. DSDP*, 21: Washington (U.S. Govt. Printing Office), 541–573.

Wentworth, C. K., 1922. A scale of grade and class terms of clastic sediments. *J. Geol.*, 30:377–390.

Williams, G. L., 1977. Dinocysts: their palaeontology, biostratigraphy and palaeoecology. *In* Ramsey, A.T.S. (Ed.), *Oceanic Micropalaeontology*: London (Academic Press), 1231–1325.

Williams, G. L., and Bujak, J. P., 1985. Mesozoic and Cenozoic dinoflagellates. *In* Bolli, H. M., Saunders, J. B., and Perch-Neilsen, K. (Eds.), *Plankton Stratigraphy*: Cambridge (Cambridge Univ. Press), 847–964.

Wise, S. W., 1983. Mesozoic and Cenozoic calcareous nannofossils recovered by Deep Sea Drilling Project Leg 71 in the Falkland Plateau region, southwest Atlantic Ocean. *In* Ludwig, W. J., Krasheninnikov, V. A., et al., *Init. Repts. DSDP*, 71: Washington (U.S. Govt. Printing Office), 481–550.

Ms 119A-103

APPENDIX A
Classification of Granular Sediments

Principal Names

Each granular-sediment class has a unique set of principal names. For pelagic sediment, the principal name describes the composition and degree of consolidation using the following terms:

1. Ooze: unconsolidated calcareous and/or siliceous pelagic sediments.
2. Chalk: firm pelagic sediment composed predominantly of calcareous pelagic grains.
3. Limestone: hard pelagic sediment composed predominantly of calcareous pelagic grains.
4. Radiolarite, diatomite, and spiculite: firm pelagic sediment composed predominantly of siliceous radiolarians, diatoms, and sponge spicules, respectively.
5. Chert: hard pelagic sediment composed predominantly of siliceous pelagic grains.

For calciclastic sediment, the principal name describes the texture and fabric, using the following terms (from Dunham, 1962):

1. Boundstone: components organically bound during deposition.
2. Grainstone: grain-supported fabric, no mud, grains <2 mm.
3. Packstone: grain-supported fabric, with intergranular mud, grains <2 mm.
4. Wackestone: mud-supported fabric, with <10% grains, grains <2 mm.
5. Calcilutite: mud-supported fabric, with >10% grains.
6. Floatstone: matrix-supported fabric, grains >2 mm.
7. Rudstone: grain-supported fabric, grains >2 mm.

For siliciclastic sediment, the principal name describes the texture and is assigned according to the following guidelines:

1. The Udden-Wentworth grain-size scale (Wentworth, 1922; Table 2) defines the grain-size ranges and the names of the textural groups (gravel, sand, silt, and clay) and subgroups (fine sand, coarse silt, etc.) that are used as the principal names of siliciclastic sediment.
2. When two or more textural groups or subgroups are present in a siliciclastic sediment, they are listed as principal names in order of increasing abundance (Shepard, 1954; Fig. 7).
3. The suffix *-stone* can be affixed to the principal names *sand, silt*, and *clay* when the sediment is lithified; *shale* is a principal name for a lithified and fissile siltstone or claystone. *Mudstone* is used for indurated, nonfissile, sandy and silty, fine-grained, siliciclastic sediments (such characteristics preclude grain-size analysis). *Conglomerate* and *breccia* are used as principal names of gravels with well-rounded and angular clasts, respectively.
4. For a poorly sorted or nonsorted clastic sediment that includes a gravel component the terms *diamicton* (unlithified), *diamictite* (lithified), and *diamict* (embracing both) are used. Such material is defined as (modified from Flint et al., 1960): "a nonsorted or poorly sorted terrigenous sediment or sedimentary rock that contains a wide range of particle sizes, such as a rock with gravel in a sandy, silty and/or clayey matrix." We defined diamict(on/ite) as containing at least 1% gravel. It becomes a breccia or conglomerate if the gravel clasts are >50%. The proportions of the individual size components should still be described. Many diamicts contain clasts in all shape categories and have mixed clast lithologies. Typical sediments are tills and debris flows.

For volcaniclastic sediment, the principal name describes the texture. The names and ranges of three textural groups (from Fisher and Schmincke, 1984) are as follows:

1. Volcanic breccia: pyroclasts >64 mm in diameter.
2. Volcanic lapilli: pyroclasts between 2 and 64 mm in diameter.
3. Volcanic ash: pyroclasts <2 mm in diameter. (When lithified, use the name *tuff*.)

Clastic sediments of volcanic provenance are described in the same fashion as siliciclastic sediments, noting the dominant composition of volcanic grains.

For mixed sediment, the principal name describes the degree of consolidation, using the terms *mixed sediments* or *mixed sedimentary rocks*. However, during Leg 119 we avoided these terms and used the principal component when it was <60% of the bulk sediment. This conveys more accurately the sediment composition.

Major and Minor Modifiers

The principal name of a granular-sediment class is preceded by major modifiers and followed by minor modifiers (preceded by the suffix *with*) that describe the lithology of the granular sediment in greater detail (Table 1).

The most common uses of major and minor modifiers are to describe the composition and textures of grain types that are present in major (>25%) and minor (10%–25%) proportions. In addition, major modifiers can be used to describe grain fabric, grain shape, and sediment color. The nomenclature for the major and minor modifiers is outlined below.

The composition of pelagic grains can be described with the major and minor modifiers *diatom*(-aceous), *radiolarian, spicules*(-ar), *siliceous, nannofossil, foraminifer*(-al), and *calcareous*. The terms *siliceous* and *calcareous* are used generally to describe sediments composed of siliceous or calcareous pelagic grains of uncertain origins.

The composition of calciclastic grains can be described with the following major and minor modifiers:

1. Ooid: spherical or elliptical nonskeletal particles <2 mm in diameter, having a central nucleus surrounded by a rim with concentric or radial fabric (oolite is used for a sediment composed mainly of ooids).
2. Bioclast (or bioclastite): fragment of skeletal remains (specific names such as molluscan or algal can also be used).
3. Pellet(-al): fecal particles from deposit-feeding organisms.
4. Intraclast: reworked rock fragment or rip-up clast.
5. Pisolith: spherical or ellipsoidal nonskeletal particle, commonly >2 mm in diameter, with or without a central nucleus but displaying multiple concentric layers of carbonate (pisolith is used for a sediment consisting mainly of pisoliths).
6. Peloid: micritized carbonate particle of unknown origin.
7. Calcareous, dolomitic, aragonitic, sideritic: used to describe the composition of carbonate muds or mudstones (micrite) of nonpelagic origins.

The texture of siliciclastic grains is described by the major and minor modifiers *gravel, sand, silt*, and *clay*.

The composition of siliciclastic grains can be described by

1. Mineralogy: using modifiers such as *quartz, feldspar, glauconite, mica, kaolinite, zeolitic, lithic* (for rock fragments), *calcareous, gypsiferous*, or *sapropelic* (for detrital clasts of calcium carbonate, gypsum, and organic matter, respectively).
2. Provenance: the source of rock fragments (particularly in gravels, conglomerates, and breccias) described by modifiers such as *volcanic, sed-lithic, meta-lithic, gneissic, basaltic*, etc.

The composition of volcaniclastic grains is described by the major and minor modifiers *lithic* (rock fragments), *vitric* (glass and pumice), and *crystal* (mineral crystals), or by modifiers that describe the compositions of the liths and crystals (e.g., *feldspar* or *basaltic*).

The fabric of the sediment can be described as grain-supported, matrix-supported, and imbricated. Generally, fabric descriptors are applied only to gravels, conglomerates, and breccias, because they provide useful information on the transport history of the sediments.

The shapes of grains are described as rounded, subrounded, subangular, and angular.

The color of sediment has been determined with a standard color-comparator, the Munsell Chart.

Chemical sediments such as salt were found.

For a description of sedimentary structures, see Figure 5.

Appendix B
Procedures to Describe Extrusives and Dikes

Enter leg, site, hole, core number and type, and section information. Draw the graphic representation of the core; number the rock pieces; and record positions of shipboard samples.

Subdivide the core into lithologic units, using the criteria of changing grain size, occurrence of glassy margins, and changes in petrographic type and phenocryst abundances.

Each lithologic unit requires the following:

1. Enter interval (consecutive downhole), including piece numbers of top and bottom pieces in unit.
2. Rock name (to be filled in last).
3. Contact type (e.g., intrusive, discordant, depositional, etc.). Note the presence of glass and its alteration products (in %); give the azimuth and dip of the contact.
4. Phenocrysts: determine if homogeneous or heterogeneous distribution; if heterogeneous distribution, note variations.

   For each phenocryst phase determine the following:

   a. Abundance (%).
   b. Average size in mm.
   c. Shape.
   d. Percent degree of alteration and replacing phases and their relationships.
   e. Further comments.
   f. Fill in 2, rock name.

5. Groundmass texture: glassy, microcrystalline, fine grained (<1 mm), medium grained (1–5 mm), or coarse grained (>5 mm). Note the relative grain-size changes within the unit (e.g., coarsening from Piece 1 to Piece 5).
6. Color (dry).
7. Vesicles: give percent, size, shape, and fillings and their relationships and distribution.
   Miaroles: give percent, size, shape, and distribution.
8. Structure: massive, pillow lava, thin flow, breccia, etc., and comments.
9. Alteration: fresh (2%), slightly (2%–10%), moderately (10%–40%), highly (40%–80%), very highly (80%–95%), or completely (95%–100%) altered.
   Type, form, and distribution of alteration.
10. Veins/Fractures: width, orientation, fillings and relationships, and halos.

Appendix C
Radiolarian Zones

Zone NR 1 = *Antarctissa denticulata* Zone Chen
Top: Holocene
Bottom: Last occurrence of *Stylatcactus universus* (0.42 Ma)

Zone NR 2 = NR2 Zone of Caulet, in part, and *S. universus* Zone of Chen, in part
Top: Last occurrence of *S. universus*
Bottom: Last occurrence of *Phormostichoartus pitomorphus*

Zone NR 3/4 = NR3 + NR4 Zone of Caulet, in part, and *Saturnalis circularis* Zone of Chen, in part
Top: Last occurrence of *P. pitomorphus*
Bottom: Last occurrence of *Clathrocyclas bicornis*. The limit between NR3 and NR4 is not yet established in Kerguelen Plateau material.

Zone NR 5 = *Eucyrtidium calvertense* Zone of Chen, in part
Top: Last occurrence of *C. bicornis*
Bottom: Last occurrence of *Prunopyle titan* (3.2 Ma)

Zone NR 6 = *Pseudocubus vema* Zone of Chen, in part
Top: Last occurrence of *P. titan*
Bottom: Evolutionary transition between *Helotholus praevema* and *P. vema*

Zone NR 7 = *Desmospyris spongiosa* Zone of Weaver and *P. vema* Zone of Chen, in part
Top: First appearance of *P. vema*
Bottom: First occurrence of *D. spongiosa* (4.25 Ma)

Zone NR 8 = *Triceraspyris coronata* Zone of Weaver and *P. vema* Zone of Chen, in part
Top: First occurrence of *D. spongiosa*
Bottom: Last occurrence of *Stichocorys peregrina* (4.5 Ma)

Zone NR 9 = *Stichocorys peregrina* Zone of Weaver and *P. vema* Zone of Chen, in part
Top: Last occurrence of *S. peregrina*
Bottom: First occurrence of *S. peregrina* (6 Ma)

Zone NR 10 = *Theocalyptra bicornis spongothorax* Zone of Chen, in part
Top: First occurrence of *S. peregrina*
Bottom: First occurrence of *T. b. spongothorax*

Zone NR 11 = *Antarctissa conradae* Zone of Chen + *Actinomma tanyacantha* Zone of Chen
Top: First occurrence of *T. b. spongothorax*
Bottom: First occurrence of *A. tanyacantha*

Zone NR 12 = *Calocyclas polyporos* Zone of Chen
Top: First occurrence of *A. tanyacantha*
Bottom: First occurrence of *C. polyporos*

Zone NR 13 = *Spongomelissa dilli* Zone of Chen
Top: First occurrence of *C. polyporos*
Bottom: First occurrence of *S. dilli*

Zone NR 14 = *Eucyrtidium punctatum* Zone of Chen
Top: First occurrence of *S. dilli*
Bottom: First occurrence of *E. punctatum*

Zone NR 15 = *Lophocyrtis regipileus* Zone of Chen
Top: First occurrence of *E. punctatum*
Bottom: First occurrence of *L. regipileus*

Zone NR 16 = *Cyrtocapsella tetrapera* Zone of Chen
Top: First occurrence of *L. regipileus*
Bottom: ?